

An efficient quantum state verification framework and its application to bosonic systems

Varun Upreti and Ulysse Chabaud

DIENS, École Normale Supérieure, PSL University, CNRS, INRIA, 45 rue d’Ulm, Paris, 75005, France

Modern quantum devices are highly susceptible to errors, making the verification of their correct operation a critical problem. Usual tomographic methods rapidly become intractable as these devices are scaled up. In this paper, we introduce a general framework for the efficient verification of large quantum systems. Our framework combines robust fidelity witnesses with efficient classical post-processing to implement measurement back-propagation. We demonstrate its usefulness by focusing on the verification of bosonic quantum systems, and developing efficient verification protocols for large classes of target states using the two most common types of Gaussian measurements: homodyne and heterodyne detection. Our protocols are semi-device independent, designed to function with minimal assumptions about the quantum device being tested, and offer practical improvements over previous existing approaches. Overall, our work introduces efficient methods for verifying the correct preparation of complex quantum states, and has consequences for calibrating large quantum devices, witnessing quantum properties, supporting demonstrations of quantum computational speedups and enhancing trust in quantum computations.

1 Introduction

Over the last years, the question of “quantum computational supremacy” or “quantum speedup” [1–3], the ability of quantum computers to outperform their classical counterparts, has given rise to a very active field of research.

ulysse.chabaud@inria.fr

Along with the theoretical development of quantum algorithms such as Shor’s algorithm [4], sub-universal quantum models such as boson sampling [5] and others [6–10] have been introduced to obtain a demonstration of quantum computational speedup in the near-term. Experimental demonstrations of quantum speedup are of paramount importance as a proof-of-principle milestone for the development of quantum computers [3, 11]. Such a demonstration requires building a quantum device to implement a desired quantum algorithm. For sub-universal quantum models, this has been achieved using random superconducting circuits [12], Fock boson sampling and optical Gaussian boson sampling [13–16]. Once such a quantum device is built, verifying its correct functioning becomes imperative: quantum devices are subject to inevitable environmental interactions that introduce errors [17]. Although fault-tolerant quantum computing offers a potential remedy, it demands a substantial resource overhead [18]. Moreover, the possibility of the quantum device behaving adversarially cannot be overlooked, e.g., in the context of delegated quantum computing [19]. Consequently, it is crucial to devise methods that rigorously ensure that the quantum device functions as intended. This task is usually referred to as *quantum verification* or *quantum certification* [20].

The task of verification can be abstractly modeled by a *prover* and a *verifier*. The prover holds a powerful device, a quantum device here, which is untrusted, whereas the verifier holds a trusted device with limited computational power. The verifier assigns a specific computational task to the prover and evaluates the prover’s trustworthiness, potentially through several rounds of interaction. It is important to note that although this verification model originates from a cryptographic interaction between two parties, it can similarly represent the calibration or certification

arXiv:2411.04688v1 [quant-ph] 7 Nov 2024

of a physical experiment, where the experiment acts as the prover and the experimentalist serves as the verifier. Making assumptions on the prover then amounts to choosing a noise model for the experiment.

In quantum physics experiments, verification is done using classical computations from samples taken from an output probability distribution describing the experiment. However, general-purpose techniques for verification such as quantum tomography rapidly become impractical for large quantum systems [21, 22]. To restore efficiency, assumptions can be made on the prover, like restricting its computational capabilities or assuming it follows a specific behavior. An important assumption is that the different copies of the quantum state produced by the experiment are i.i.d. (independent and identically distributed). This i.i.d. assumption can be removed, by paying the cost of an associated overhead in the number of samples [23, 24].

What defines a good verification protocol depends of course on the exact setting, but one generally aims to minimize the complexity of the verifier, the complexity of the prover, the assumptions made on the prover’s behavior, and the number of samples required [25]. In addition, for quantum physics experiments, a meaningful figure of merit for verification is based on the total variation distance between a target probability distribution and the true distribution describing the functioning of the device, as it bears operational significance.

Significant strides have been made in the efficient verification of universal quantum computation over the past few years [24, 26, 27]. In contrast, there is a noticeable lack of robust verification protocols for sub-universal quantum models, such as boson sampling. This difficulty in verification is primarily due to the anti-concentration of target probability distributions across an exponentially large sample space. Moreover, the verification methods that utilize total variation distance and presume the verifier can only perform classical computations either rely on poorly understood assumptions [7, 28, 29] or introduce complex protocols that limit their practical use in current experiments [27, 30, 31].

For approaches that require fewer resources, one may opt for partial verification techniques [9, 12, 32–34]. In these methods, instead of eval-

uating the total variation distance, specific characteristics of the experimental probability distribution are examined. These techniques are contingent upon certain assumptions regarding the operational mechanisms of the quantum device [35]. Alternatively, one may require the verifier to possess only basic quantum computational abilities. In this scenario, the verifier’s objective is to assess how closely the state generated by the prover aligns with a predetermined target state, which in turn provides insights into the similarity between the actual and target probability distributions. This can be performed through fidelity estimation or the application of a fidelity witness, which serves as a lower bound on the fidelity between the two states [36–39].

Continuous-variable quantum systems, where quantum states live in an infinite-dimensional Hilbert space [40, 41], have emerged as a promising alternative to discrete-variable systems due to their suitability for photonics, the regime boson sampling falls into, with unprecedented levels of entanglement achieved experimentally [42], but also for bosonic quantum error correction [43–45]. In the context of continuous-variable quantum systems, Gaussian state preparation and measurements are basic operations: they have been the subject of considerable theoretical investigation [46] and lead to computations that can be simulated classically [47]; moreover, they can be implemented experimentally on a large scale [42, 48, 49]. Nevertheless, there remains a significant gap concerning efficient verification protocols based on such Gaussian operations. Existing protocols [50–53] suffer from experimental impracticality either due to exponential scaling [50, 52] or limited robustness [51, 53], i.e., the verification method used require a high value of the true fidelity between the target and experimental state to guarantee any meaningful information.

In this work, we introduce a general framework for the efficient verification of large quantum systems based on robust fidelity witnesses and efficient classical post-processing. We apply this framework to bosonic quantum systems and derive semi-device independent verification protocols based on Gaussian homodyne or heterodyne measurements, which are both efficient and robust, addressing current limitations of existing protocols. These provide a robust alternative to [51] for verifying the output states of quantum

speedup experiments such as boson sampling, and can be used more generally to calibrate or certify efficiently a wide variety of large-scale quantum devices.

The rest of the paper is organized as follows: we provide preliminary material in section 2, and detail our framework for efficient verification in section 3. This framework is based on robust fidelity witnesses, and we introduce a general family of such witnesses in section 4, of which we study the robustness from both analytical and numerical points of view. Then, we apply our framework to derive new efficient verification protocols for bosonic systems: in section 5, we first introduce efficient verification protocols based on homodyne detection and existing fidelity witnesses; then, in section 6, we describe verification protocols with heterodyne sampling utilizing our new fidelity witnesses, and show in particular that they allow for verifying a large class of non-Gaussian states known as doped Gaussian states [54]. As a byproduct, in section 7 we give a detailed comparison of heterodyne and homodyne detection in the context of continuous-variable quantum verification protocols. Finally, we conclude in section 8.

2 Preliminaries

We refer the reader to [55] for background on quantum information theory tools used in this work, and to [40, 41, 49] for continuous-variable quantum information material.

Hereafter, the sets \mathbb{N}, \mathbb{R} and \mathbb{C} are the set of natural, real, and complex numbers respectively, with a $*$ exponent when 0 is removed from the set, $m \in \mathbb{N}^*$ denotes the number of modes and $\{|n\rangle\}$ is the single-mode Fock basis. Single-mode displacement operators and single-mode squeezing operators are defined as $\hat{D}(\alpha) = e^{\alpha\hat{a}^\dagger - \alpha^*\hat{a}}$ and $\hat{S}(\xi) = e^{\frac{1}{2}(\xi\hat{a}^2 - \xi^*\hat{a}^{\dagger 2})}$ respectively, where $\alpha, \xi \in \mathbb{C}$ and \hat{a}, \hat{a}^\dagger denote the annihilation and creations operator, respectively [41]. Finally, we use bold math notations for vectors, multimode states, and multi-index notations. For all $\boldsymbol{\beta}, \boldsymbol{\xi} \in \mathbb{C}^m$, we write $\hat{D}(\boldsymbol{\beta}) = \otimes_{i=1}^m \hat{D}(\beta_i)$ and $\hat{S}(\boldsymbol{\xi}) = \otimes_{i=1}^m \hat{S}(\xi_i)$. Passive linear quantum operations play an important role in the paper. A passive linear quantum operation is a Gaussian transformation which preserves the total energy or photon number of a system. Common examples include beam split-

ters and phase shifters.

The position and momentum operators are referred to as the quadrature operators, and are given by

$$\hat{q} = \frac{1}{\sqrt{2}}(\hat{a} + \hat{a}^\dagger), \quad (1)$$

$$\hat{p} = \frac{1}{i\sqrt{2}}(\hat{a} - \hat{a}^\dagger), \quad (2)$$

where \hat{q}, \hat{p} refer to the position and momentum quadrature operator respectively. They follow the canonical commutation relation $[\hat{q}, \hat{p}] = i\mathbb{1}$ (with the convention $\hbar = 1$). Finally, a rotated quadrature is given by

$$X_\theta = \frac{1}{\sqrt{2}}(\hat{a}e^{-i\theta} + \hat{a}^\dagger e^{i\theta}). \quad (3)$$

Operations that transform a Gaussian state into a Gaussian state are called Gaussian operations. The most common Gaussian measurements are heterodyne detection, which projects the state onto a coherent state and correspond to sampling from the Husimi Q function; and homodyne detection, which correspond to the measurement of a rotated quadrature operator.

The fidelity gives a measure of the closeness of two quantum states ρ and σ and is defined as

$$F(\rho, \sigma) = \text{Tr} \left[\sqrt{\sqrt{\sigma}\rho\sqrt{\sigma}} \right]^2. \quad (4)$$

Despite it not being apparent, $F(\rho, \sigma)$ is symmetric in ρ and σ . When one of the states is pure, the expression reduces to $F(|\psi\rangle, \rho) = \text{Tr}[|\psi\rangle\langle\psi|\rho] = \langle\psi|\rho|\psi\rangle$ and in particular when both states are pure, $F(|\psi\rangle, |\phi\rangle) = |\langle\phi|\psi\rangle|^2$.

The total variation distance between two probability distributions P and Q over a continuous sample space Ω is a measure of how different the two distributions are. It is defined as

$$d_{TV}(P, Q) = \frac{1}{2} \int_{x \in \Omega} |P(x) - Q(x)| dx. \quad (5)$$

The trace distance between two states ρ, σ is given by

$$D(\rho, \sigma) = \frac{1}{2} \text{Tr}(|\rho - \sigma|), \quad (6)$$

and satisfies $D(\rho, \sigma) = \max_{\hat{O}} \|P_\rho^{\hat{O}} - P_\sigma^{\hat{O}}\|_{\text{tvd}}$. The probability distribution $P_\rho^{\hat{O}}$ (and similarly $P_\sigma^{\hat{O}}$) arises from measuring observable \hat{O} on states ρ

and σ , with the maximum total variation distance taken over all observables. Two states being close in trace distance thus indicates that quantum computations using either state as input will yield nearly identical results. Finally, the fidelity and trace distance are related by the Fuchs-van de Graaf inequalities [56]

$$1 - \sqrt{F(\rho, \sigma)} \leq D(\rho, \sigma) \leq \sqrt{1 - F(\rho, \sigma)}. \quad (7)$$

Therefore, knowledge of the fidelity between two states gives a bound on the trace distance between them.

The efficiency of fidelity estimation protocols between a measured state and a target state depend on the number of measurements performed. The fidelity can be written as a classical expectation value of estimator functions over these measurement outcomes, and with a finite number of samples N , we use Hoeffding's inequality [57] to estimate the closeness of the average estimator values calculated from these samples to the expectation value of the estimators.

Lemma 1 (Hoeffding's inequality). *Let $\epsilon > 0$, let $n \geq 1$, let z_1, \dots, z_n be i.i.d. complex random variables from a probability density D over \mathbb{R} , and let $g : \mathbb{C} \rightarrow \mathbb{R}$ be a bounded function and let $G \geq \max g(z) - \min g(z)$. Then*

$$\Pr \left(\left| \frac{1}{N} \sum_{i=1}^N g(z_i) - \mathbb{E}_{z \leftarrow D}[g(z)] \right| \geq \epsilon \right) \leq 2 \exp \left(-\frac{2N\epsilon^2}{G^2} \right). \quad (8)$$

3 Verification framework

In this section, we introduce a general framework for efficient verification of quantum states, which we base our protocols on.

In general, verifying the correct preparation of a state $|\psi\rangle$ through tomography requires exponentially many measurements [21]. However, quantum verification methods which focus on specific classes of states may achieve exponentially better sample complexity, as we demonstrate hereafter. Suppose we want to verify the fidelity of an unknown state ρ with a target state $|\psi\rangle$, by making measurements whose positive operator-valued measure (POVM) elements are denoted $\{\Pi_\lambda\}_\lambda$. In our framework, an efficient verification protocol combines two ingredients (see Figure 1):

1. **Efficient and robust fidelity witness:** For an unknown state ρ and a class of target states $\{|\psi\rangle\}$, we require a fidelity witness $W(\rho, \psi)$ that is efficiently computable using samples from the measurement described by $\{\Pi_\lambda\}_\lambda$ and that is robust, i.e., that satisfies an equation of the form:

$$f(F) \leq W(\rho, \psi) \leq F(\rho, \psi), \quad (9)$$

where f is a continuous function such that $f(1) = 1$. The inequality on the right-hand side indicates that the fidelity witness is indeed a lower bound on the fidelity $F(\rho, \psi)$, whereas the left-hand side gives the range of fidelity where the fidelity witness provides meaningful information, i.e., where $W(\rho, \psi) \geq 0$.

2. **Measurement back-propagation:** To extend the class of states which can be verified efficiently, we use efficient classical post-processing of measurement samples to simulate undoing the effects of a unitary operation before the measurement. Denoting such a set of unitaries as $\{\hat{U}_\mu\}_\mu$, this is possible when the POVM elements Π_λ of the measurement device satisfy the following condition:

$$\hat{U}_\mu \Pi_\lambda \hat{U}_\mu^\dagger = \Pi_{g_\mu(\lambda)}, \quad (10)$$

where $g_\mu(\lambda)$ is an invertible function of λ for all μ which can be computed efficiently.

The first point allows us to verify efficiently the correct preparation of a target state $|\psi\rangle$, by estimating the value of the fidelity witness using measurement outcomes from the POVM $\{\Pi_\lambda\}_\lambda$. The second point allows us to extend the efficient verification to all the states of the form $\hat{U}_\mu |\psi\rangle$ with classical post-processing, since

$$\text{Tr}[\rho \Pi_{g_\mu(\lambda)}] = \text{Tr}[\hat{U}_\mu^\dagger \rho \hat{U}_\mu \Pi_\lambda]. \quad (11)$$

This means that measuring ρ with the POVM $\{\Pi_\lambda\}_\lambda$ and post-processing the measurement outcomes as $\lambda \mapsto g_\mu(\lambda)$ effectively emulates the application of the quantum operation U_μ^\dagger on ρ before the measurement, and reduces the verification of $\hat{U}_\mu |\psi\rangle$ to the verification of $|\psi\rangle$.

This framework is applicable to both discrete-variable and continuous-variable quantum systems and relies on the availability of robust fidelity witnesses. In the next section, we introduce a family of such fidelity witnesses, for arbitrary *separable* target states. Then, in the rest of

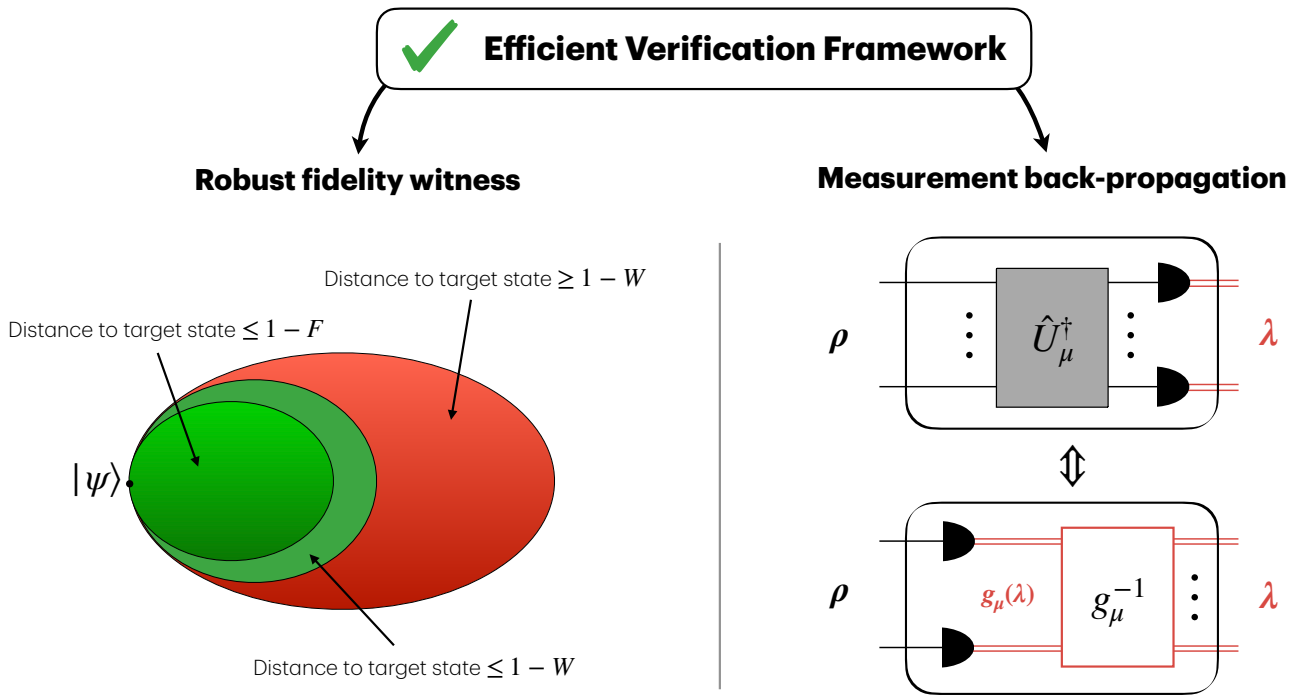


Figure 1: Concepts behind our efficient verification framework. Any verification protocol combining efficient and robust fidelity witnesses for a class of target states with measurement back-propagation for emulating quantum operations before the measurements can be used to efficiently verify a larger class of target states. The right hand side depicts the information retrieved by estimating a fidelity witness. The left hand side represents measurement back-propagation: in black are quantum operations and measurements and in red classical measurement outcomes and operations.

the paper, we focus on continuous-variable verification protocols combining these new fidelity witnesses with efficient classical post-processing to efficiently verify large classes of continuous-variable quantum states, and overcome limitations of existing Gaussian verification protocols.

4 Robust fidelity witnesses

In this section, we introduce a family of fidelity witnesses for arbitrary separable target states and provide analytical and numerical analyses of their robustness.

4.1 Fidelity witnesses based on k -mode fidelities

We consider a m -mode quantum systems, and we assume that m is divisible by k . For two m -mode quantum states ρ and $|\psi\rangle$, let us define the following multimode fidelity witness for an m -mode

system:

$$W^{(k)}(\rho, \psi) := 1 - \sum_{i=1}^{m/k} [1 - F(\rho_{i;k}, |\psi_{i;k}\rangle)], \quad (12)$$

where $\sigma_{i;k} := \text{Tr}_{\{1, \dots, m\} \setminus \{ki-(k-1), \dots, ki\}}[\sigma]$ denotes the reduced state over the i^{th} subset of k modes $\{ki - (k - 1), \dots, ki\}$. Note that the choice of modes is for brevity, and one can similarly define witnesses based on any other partition of m modes into subsets of k modes, or even based on a partition into subsets of modes of different sizes. Setting $k = 1$ retrieves a witness based on single-mode fidelities previously introduced in [51], while setting $k = m$ retrieves the m -mode fidelity.

Intuitively, one may think that the witness in Eq. (12) provides a better bound on the fidelity as k increases, since we are losing less information by tracing out some of the modes. This intuition is formalized by the following result:

Lemma 2 (Robustness of fidelity witnesses). *Let ρ and $|\psi\rangle$ be states over m subsystems. Then for*

all $k \in \{1, \dots, m\}$,

$$W^{(1)}(\rho, \psi) \leq W^{(k)}(\rho, \psi), \quad (13)$$

and

$$1 - \frac{m}{k}(1 - F(\rho, |\psi\rangle)) \leq W^{(k)}(\rho, \psi) \leq F(\rho, |\psi\rangle). \quad (14)$$

We direct the reader to sections A of the appendix for the proof.

Eq. (14) shows that $W^{(k)}(\rho, \psi)$ gives us a lower bound of the fidelity between ρ and $|\psi\rangle$, whereas Eq. (13) proves $W^{(k)}(\rho, \psi)$ is a better lower bound of the fidelity than $W^{(1)}(\rho, \psi)$. In addition $W^{(k)}(\rho, \psi)$ requires fidelity $F(\rho, |\psi\rangle) > 1 - k/m$ to guarantee meaningful information, i.e., $W^{(k)}(\rho, \psi) > 0$. Therefore, $W^{(k)}(\rho, \psi)$ is more robust than $W^{(1)}(\rho, \psi)$ for $k > 1$. On the other hand, $W^{(k)}(\rho, \psi)$ requires the estimation of k -mode fidelities, which has sample complexity exponential in k in general.

Given this trade-off between robustness and sample complexity, it is beneficial in practical applications to identify scenarios where employing a multimode fidelity witness offers a clear advantage. We address this problem through numerical examples in the next section.

4.2 Numerical analysis

In this section, we illustrate the robustness of the fidelity witnesses defined in Eq. (12) through numerical analysis of three examples. In the first example, the deviation of the tested state from the target state is essentially random, while in the two other examples, the deviation has structure, reflected in the robustness of the corresponding witnesses.

Example 1: We start by the following example: the target state $|\psi\rangle = \hat{U}|1\rangle^{\otimes 6}$ is chosen as the output state of a 6-mode Boson Sampling experiment, i.e., a Fock state passing through a lossless passive linear interferometer described by the unitary \hat{U} . The tested state is a lossy and noisy version of the target state: it first undergoes equal single-mode losses, represented as a six-mode channel \mathcal{L}_η , where η is a loss parameter (the lossless case corresponding to $\eta = 1$) followed by a slightly perturbed interferometer \hat{U}' instead of the ideal \hat{U} , such that $\hat{V} := \hat{U}'\hat{U}^\dagger \approx \hat{\mathbb{1}}$ is a small random passive linear unitary imperfection. Consequently, after the classical post-processing step,

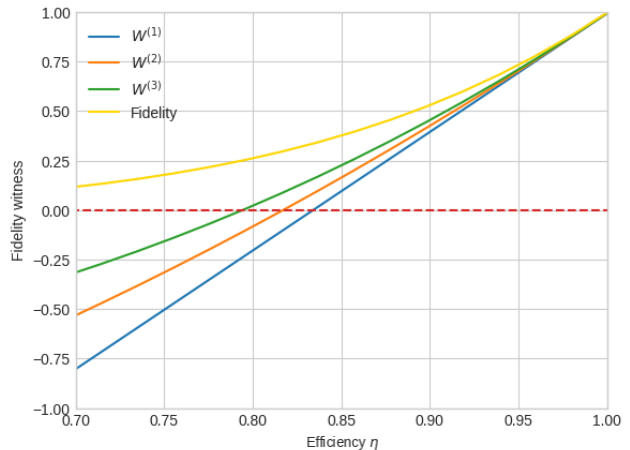
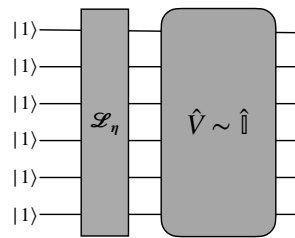


Figure 2: (Top) Quantum circuit considered in the analysis given in Example 1 of section 4.2. (Bottom) Fidelity witnesses based on single-mode, two-mode, and three-mode fidelities as a function of the loss parameter η . For each value of η , we average over different choices of unitary interferometer deviations \hat{V} that are close to identity. For a fidelity witness to be useful, it needs to take positive values. The fidelity witness based on two-mode fidelities is useful for the largest range of single-mode loss parameter values, followed by the witness based on two-mode fidelities, and finally by the one based on single-mode fidelities.

instead of achieving the target state $|\psi\rangle$, we obtain the noisy state $\hat{V}\mathcal{L}_\eta(|\psi\rangle\langle\psi|)\hat{V}^\dagger$.

Varying the loss parameter η from 0 to 1 and for each value of η , averaging over a family of unitary interferometer imperfections \hat{V} that are close to identity, we analyze the performance of single-mode, two-mode, and three-mode fidelity witnesses as a function of η . The results are presented in Figure 2. As expected, the fidelity witness based on three-mode fidelities remains positive over a larger range of η , meaning it remains effective over a wider span of losses compared to the witnesses based on two-mode and single-mode fidelities, respectively.

This example illustrates that, in cases with single-mode losses followed by random close-to-

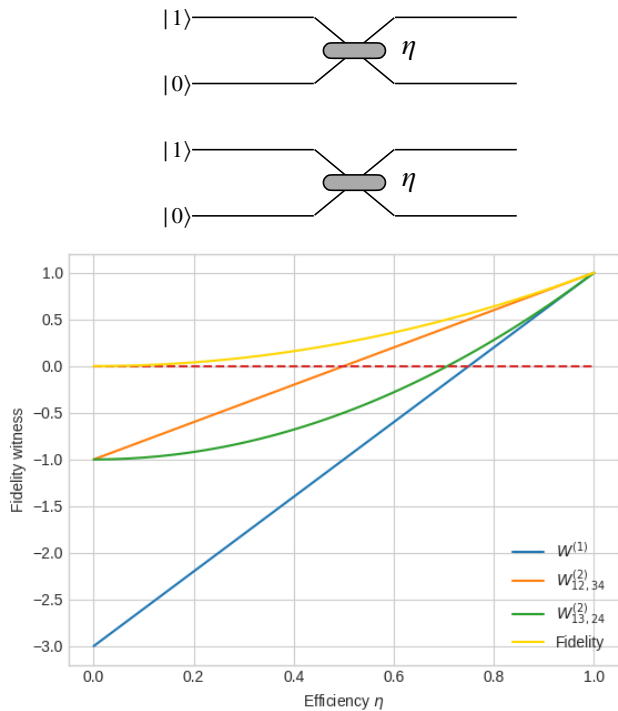


Figure 3: (Top) Quantum circuit considered in the analysis given in Example 2 of Section 4.2. (Bottom) Comparison of the two-mode fidelity witnesses for the circuit given. The two-mode fidelity witness where the modes 1, 2 and 3, 4 are paired up is the closest to the actual value of fidelity, mimicking the noise structure.

identity interferometers, the utility of the three-mode or two-mode fidelity witnesses marginally surpasses that of the single-mode fidelity witness. Because of the random deviation, the pairing of the modes does not affect the quality of the witnesses. However, in practical scenarios where systematic errors are present, different pairings of modes can yield different information (and thus distinct fidelity witness values), due to the structure of the deviation of the tested state from the target state. This feature can be useful to characterize the noise structure within a device and exploit it for efficient verification. To illustrate this point, we consider two additional examples.

Example 2: We consider a two-mode state, $|1010\rangle$, passing through two beamsplitters with efficiency η , applied between modes 1 and 2, and modes 3 and 4. With the target state being $|1010\rangle$ ($\eta = 1$), we compare the actual value of fidelity between the target state and the output state of this circuit with fidelity witnesses based on two-mode fidelities for pairs (1,2) and (3,4) ($W_{12,34}^{(2)}$),

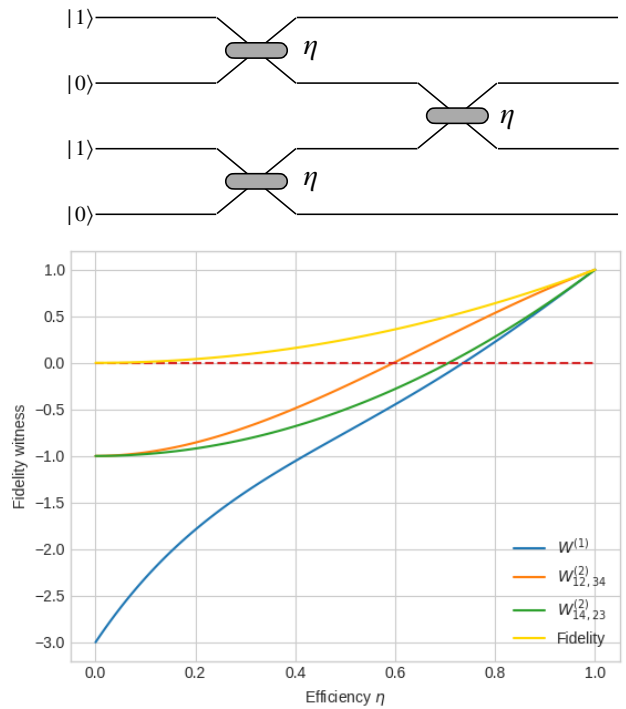


Figure 4: (Top) Quantum circuit considered in the analysis given in Example 3 of Section 4.2. (Bottom) Comparison of the two-mode fidelity witnesses and single-mode fidelity witness for the circuit given. Two-mode fidelity witness which pairs more entangled modes gives a better estimate of the fidelity.

and for pairs (1,3) and (2,4) ($W_{13,24}^{(2)}$), and on single-mode fidelities (Figure 3). When modes affected by correlated noise are grouped as pairs, the two-mode fidelity witnesses align more closely with the actual fidelity. This suggests that selecting pairs which accurately capture the correlation structure of the noise yields a better fidelity lower bound. In scenarios where pairing all correlated modes is not feasible, choosing fidelity witnesses that capture as much entanglement as possible remains the optimal approach.

Example 3: The last example we consider closely mirrors the previous one, with the input state changed from $|1010\rangle$ to $|1001\rangle$, and an additional beamsplitter entangling modes 2 and 3. With the target state being $|1001\rangle$ ($\eta = 1$), we compare the actual value of fidelity between the target state and output state of this circuit with the fidelity witnesses based on two-mode for pairs (1,2) and (3,4) ($W_{12,34}^{(2)}$), and for pairs (1,4) and (2,3) ($W_{14,23}^{(2)}$), and on single-mode fidelities (Figure 4). In this case, there is correlated noise be-

tween modes 1 and 2, modes 3 and 4, as well as between modes 2 and 3. The two-mode fidelity witness that pairs the more strongly correlated modes, namely $W_{12,34}^{(2)}$, provides a better estimate of the fidelity.

In what follows, we illustrate the applicability of our efficient verification framework introduced in section 3, by combining the witnesses introduced in this section with efficient classical post-processing for measurement back-propagation. We consider the verification of bosonic systems based on continuous-variable quantum measurements, namely homodyne detection (section 5) and heterodyne detection (section 6).

5 Verification protocols with homodyne detection

5.1 Homodyne detection

Homodyne detection is a single-mode Gaussian measurement that mathematically corresponds to projection on the rotated quadrature operator $\hat{X}_\theta = \frac{1}{\sqrt{2}}(\hat{a}e^{-i\theta} + \hat{a}^\dagger e^{i\theta})$, and homodyne measurement on a state ρ corresponds to sampling from the probability distribution

$$P_\rho(x, \theta) = \langle x |_\theta \rho | x \rangle_\theta, \quad (15)$$

where $|x\rangle_\theta$ is an eigenstate of the quadrature operator \hat{X}_θ . Experimentally, homodyne detection is implemented by mixing an incoming signal beam with a strong local oscillator beam at the same frequency, typically using a beamsplitter. The mixed beams then interfere, and the resulting signal is measured by photodetectors. The phase and amplitude of the signal beam are inferred by adjusting the phase of the local oscillator and analyzing the difference in photodetector outputs. The positive operator valued-measure (POVM) elements of a tensor product of single-mode homodyne detection over m modes of quadrature operator at positions $\mathbf{x} = \{x_1, \dots, x_m\} \in \mathbb{R}^m$ rotated at the same angle θ are given by

$$\Pi_{\mathbf{x}} = |\mathbf{x}\rangle_\theta \langle \mathbf{x}|_\theta, \quad (16)$$

where $|\mathbf{x}\rangle_\theta$ is the eigenstate of the quadrature operator $\mathbf{X}_\theta = \frac{1}{\sqrt{2}}(\hat{\mathbf{a}}e^{-i\theta} + \hat{\mathbf{a}}^\dagger e^{i\theta})$. Since all angles are equal, we call this multimode measurement *parallel homodyne detection*.

5.2 Single-mode homodyne fidelity estimation

We now describe a protocol to estimate the fidelity between an experimental state and a single-mode target state with a finite support over the Fock basis, also known as core states [58]. We introduce homodyne estimator functions as

$$f_{lk}(x) e^{i(l-k)\theta}, \quad (17)$$

where

$$f_{lk}(x) := 4xu_k(x)v_l(x) - 2\sqrt{k+1}u_{k+1}(x)v_l(x) - 2\sqrt{l+1}u_k(x)v_{l+1}(x), \quad (18)$$

with $u_j(x)$ and $v_j(x)$ the normalizable and unnormalizable eigenfunctions of the harmonic oscillator with eigenvalue j , respectively, whose expressions are given in section B of the appendix. The notable property of these estimator functions is [59]:

$$\rho_{kl} = \mathbb{E}_{P_\rho(x, \theta)} [f_{lk}(x) e^{i(l-k)\theta}], \quad (19)$$

where the angle θ is drawn uniformly randomly. In particular, since homodyne detection corresponds to sampling from the probability distribution function $P_\rho(x, \theta)$ given by Eq. (15), Eq. (19) allows the estimation of any element k, l of the density matrix by computing the mean of the function $(x, \theta) \mapsto f_{lk}(x) e^{i(l-k)\theta}$ over these homodyne samples, for random choices of homodyne angles θ .

For any single-mode core state $|C\rangle = \sum_{n=0}^{c-1} c_n |n\rangle$, where $c \in \mathbb{N}^*$ and $x, \theta \in \mathbb{R}$, we define the function

$$g_{|C\rangle}^{(\text{hom})}(x, \theta) = \sum_{0 \leq k, l \leq c-1} c_k^* c_l f_{lk}(x) e^{i(l-k)\theta}. \quad (20)$$

Computing the mean of $g_{|C\rangle}^{(\text{hom})}$ over homodyne samples of some unknown state ρ gives us an estimate of the fidelity with the state $|C\rangle$. This leads to the following single-mode fidelity estimation protocol using homodyne detection, assuming that the different copies of ρ are *i.i.d.*, i.e., independent and identically distributed.

Protocol 1 (Single-mode fidelity estimation with homodyne detection). *Let $c \in \mathbb{N}^*$ and let $|C\rangle = \sum_{n=0}^{c-1} c_n |n\rangle$ be a core state, where $c \in \mathbb{N}^*$. Let also $N \in \mathbb{N}^*$. Let $\rho^{\otimes(N+1)}$ be $N+1$ copies of an unknown single-mode (mixed) quantum state.*

1. Measure N copies of ρ with homodyne detection at a phase θ (sampled by measuring the phase of the local oscillator), obtaining the samples $x^{(1)}, \dots, x^{(N)}; \theta^{(1)}, \dots, \theta^{(N)} \in \mathbb{R}$.
2. Compute the mean F_C of the function $(x, \theta) \mapsto g_{|C\rangle}^{(\text{hom})}(x, \theta)$ (given by Eq. (20)) over the samples $(x^{(1)}, \theta^{(1)}), \dots, (x^{(N)}, \theta^{(N)}) \in \mathbb{R}^2$.
3. F_C gives the estimate of the fidelity between the one remaining copy of ρ and $|C\rangle$.

The following theorem summarizes the efficiency of this protocol:

Theorem 1 (Efficiency of Protocol 1). *Let $\epsilon, \delta > 0$. With the notations of Protocol 1, the estimate of $F_C(\rho)$ is ϵ -close to $F(\rho, |C\rangle)$ with probability $1 - \delta$ whenever $N \geq N_1$ with*

$$N_1 = \mathcal{O} \left(\left(\frac{C^{\frac{10}{3}}}{\epsilon} \right)^2 \log \left(\frac{1}{\delta} \right) \right), \quad (21)$$

where C is the support size of the target core state.

We direct the reader to section C of the appendix for the proof, which combines Eq. (19) with Hoeffding's inequality [57].

Since N_1 scales polynomially in ϵ and logarithmically in $1/\delta$, Protocol 1 is efficient for fidelity estimation between an unknown single-mode quantum state and a core state. Since core states form a dense subset (for the trace norm) of the set of normalized single-mode pure quantum states, given any target normalized single-mode pure state $|\psi\rangle$, we can use our fidelity estimation protocol by targeting instead a truncation of the state $|\psi\rangle$ in the Fock basis in order to estimate the fidelity of any single-mode continuous-variable quantum state with the state $|\psi\rangle$ using homodyne detection. While of similar nature, our protocol differs from the one recently studied in [60], in that we perform direct fidelity estimation while their bounds apply to reconstructing a full density matrix up to some cutoff in Fock basis.

In a cryptographic scenario, the i.i.d. assumption cannot be assumed, that is, the state ρ^{N+1} sent by the quantum device may not be of the form $\rho^{\otimes(N+1)}$. Protocol 1 can be adapted to such a scenario using standard de Finetti reductions [23, 24]. From a similar method used in [51]

for heterodyne detection, one may expect that this would result in a polynomial overhead in the number of samples required for a given precision [61], likely preventing the protocol from being experimentally realizable in the near term. Therefore we do not delve into it hereafter, focusing instead on practical verification methods, under the i.i.d. assumption.

5.3 Multimode homodyne verification

In this section, we show that Protocol 1 can be extended to estimate a multimode fidelity witness, i.e., a tight lower bound on the fidelity as explained in Eq. (9), for multimode target states of the form $\hat{D}(\beta)\hat{O}^{\otimes m}|C_i\rangle$, where $|C_i\rangle$ is a core state in the i^{th} mode, and where \hat{O} is an m -mode passive linear transformation with an associated $2m \times 2m$ block diagonal orthogonal symplectic matrix S_O , which describes its action on the quadrature operators.

Given an m -mode output state ρ and a target state $|\psi\rangle = |\psi_1\rangle \otimes \dots \otimes |\psi_m\rangle$, we use the witness in Eq. (12) for $k = 1$. This witness, originally introduced in [51], is based on single-mode fidelities and given by

$$W(\rho, \psi) := 1 - \sum_{i=1}^m (1 - F(\rho_i, \psi_i)), \quad (22)$$

where $F(\rho_i, \psi_i)$ is the fidelity between $|\psi_i\rangle$ and the reduced state $\rho_i = \text{Tr}_{\{1, \dots, m\} \setminus \{i\}}[\rho]$.

By Lemma 2 with $k = 1$ (see also [51, Lemma 2]),

$$1 - m(1 - F(\rho, \psi)) \leq W(\rho, \psi) \leq F(\rho, \psi). \quad (23)$$

Therefore, W is a tight lower bound on the fidelity. Furthermore, W is a function of only single-mode fidelities. Being able to estimate single-mode fidelities with single-mode pure states using homodyne detection thus allows us to witness the multimode fidelity of an m -mode output experimental state ρ with any target pure product state using homodyne detection, by using Protocol 1 for each subsystem in parallel.

We further make use of the properties of homodyne detection to extend the class of target states for which tight fidelity witnesses can be efficiently obtained: an orthogonal passive linear transformation followed by a displacement operator before homodyne detection is equivalent to

performing the homodyne detection directly, then classically post-processing the samples obtained. Formally:

Lemma 3 (Back-propagation of parallel homodyne measurement). *Let $\beta \in \mathbb{C}^m$ and let $\hat{V} = \hat{D}(\beta)\hat{O}$, where \hat{O} is an m -mode passive linear transformation with $m \times m$ block diagonal orthogonal unitary matrix O . Let $\mathbf{x}' = (S_O)_1 \mathbf{x} + \beta_\theta$, where β_θ is the component of β along the direction defined by θ in the phase space ($\beta_\theta = \text{Re}(\beta) \cos(\theta) + \text{Im}(\beta) \sin(\theta)$) and $(S_O)_1$ is expressed by*

$$S_O = \begin{bmatrix} (S_O)_1 & \mathbf{0} \\ \mathbf{0} & (S_O)_1 \end{bmatrix}. \quad (24)$$

Then,

$$\Pi_{\mathbf{x}'_\theta} = \hat{V} \Pi_{\mathbf{x}_\theta} \hat{V}^\dagger, \quad (25)$$

where

$$\Pi_{\mathbf{x}_\theta} = |\mathbf{x}_\theta\rangle_\theta \langle \mathbf{x}_\theta|_\theta \quad (26)$$

is the POVM for parallel homodyne detection at angle θ . $|\mathbf{x}_\theta\rangle_\theta$ is the eigenstate of the quadrature operator $\mathbf{X}_\theta = \frac{1}{\sqrt{2}} (\mathbf{a} e^{-i\theta} + \mathbf{a}^\dagger e^{i\theta})$.

We direct the reader to section D of the appendix for the proof. An important implication is that a certain class of quantum operations (orthogonal passive linear operations) before a parallel homodyne detection can be inverted by doing classical post-processing on the samples of the parallel homodyne detection. In particular, for such a transformation \hat{V} , if a multimode pure product state $\otimes_{i=1}^m |\psi_i\rangle$ can be efficiently verified using parallel homodyne detection, then the state $\hat{V} \otimes_{i=1}^m |\psi_i\rangle$ can be efficiently verified using parallel homodyne detection and efficient classical post-processing.

This leads us to our multimode homodyne verification protocol:

Protocol 2. (Multimode verification with parallel homodyne detection). *Let $c_1, \dots, c_m \in \mathbb{N}^*$. Let $|C_i\rangle = \sum_{n=0}^{c_i-1} c_{i,n} |n\rangle$ be a core state, for all $i \in \{1, \dots, m\}$. Let \hat{O} be an m -mode orthogonal passive linear transformation with $m \times m$ block diagonal orthogonal matrix S_O , given by Eq. (24), and $\beta \in \mathbb{C}^m$. We write $|\psi\rangle = \hat{D}(\beta)\hat{O} \otimes_{i=1}^m |C_i\rangle$ the m -mode target pure state. Let $N \in \mathbb{N}^*$ and let $\rho^{\otimes(N+1)}$ be $N+1$ copies of an unknown m -mode (mixed) quantum state.*

1. Measure all m subsystems of N copies of ρ with parallel homodyne detection at angle θ_k ,

chosen randomly, with $k \in \{1, \dots, N\}$, obtaining the vectors of samples $\mathbf{x}'_1, \dots, \mathbf{x}'_N \in \mathbb{R}^m$.

2. For all $k \in \{1, \dots, N\}$, compute the vectors $\mathbf{x}_k = (S_O)_1^{-1}(\mathbf{x}'_k - \beta_{\theta_k})$, where $\beta_{\theta_k} = \text{Re}(\beta) \cos(\theta) + \text{Im}(\beta) \sin(\theta)$ is the component of β along the θ direction. We write $\mathbf{x}_k = (x_{1k}, \dots, x_{mk}) \in \mathbb{R}^m$.
3. For all $i \in \{1, \dots, m\}$, compute the mean F_{C_i} of the function $(x, \theta) \mapsto g_{|C_i\rangle}^{(\text{hom})}(x, \theta)$ over the samples $x_{i1}, \dots, x_{iN} \in \mathbb{R}$.
4. Compute the fidelity witness estimate $W_\psi = 1 - \sum_{i=1}^m (1 - F_{C_i})$.

W_ψ provides a lower bound on the fidelity between any m -mode (mixed) quantum state ρ and $|\psi\rangle$. The efficiency of the protocol is summarized as follows:

Theorem 2 (Efficiency of Protocol 2). *Let $\epsilon, \delta > 0$. With the notations of Protocol 2,*

$$1 - m(1 - F(\rho, |\psi\rangle)) - \epsilon \leq W_\psi \leq F(\rho, |\psi\rangle) + \epsilon \quad (27)$$

with probability greater than $1 - \delta$, whenever $N \geq N_2$, with

$$N_2 = \mathcal{O} \left(\frac{m^2}{\epsilon^2} C^{\frac{20}{3}} \log \left(\frac{m}{\delta} \right) \right), \quad (28)$$

where $C = \max_{i \in \{1, \dots, m\}} c_i$, where c_i is the support size for the core state in the mode i .

We direct the reader to section E in the appendix for the proof.

Protocol 2 provides an efficient method to estimate the fidelity between an unknown m -mode (mixed) quantum state ρ and $|\psi\rangle$, where $|\psi\rangle = \hat{D}(\beta)\hat{O} \otimes_{i=1}^m |C_i\rangle$ using homodyne sampling.

5.4 Imperfect homodyne detection

Protocols 1 and 2 are described under the assumption of unit efficiency of the homodyne detection. For an arbitrary quantum efficiency η , $f_{lk}(x)$ and $P_\rho(x, \theta)$ should be modified as [59]:

$$f_{kl}^\eta(x) = e^{i\frac{\pi}{2}(l-k)} \sqrt{\frac{k!}{l!}} \times \int_{-\infty}^{\infty} dt |t| e^{\frac{1-2\eta}{2\eta} t^2 - i2tx} t^{(l-k)} L_k^{(l-k)}(t^2), \quad (29)$$

and

$$P_\rho^\eta(x, \theta) = \sqrt{\frac{2\eta}{\pi(1-\eta)}} \times \int_{-\infty}^{\infty} dx' e^{-\frac{2\eta}{1-\eta}(x-x')^2} P_\rho(x', \theta), \quad (30)$$

where L_n^a are the generalized Laguerre polynomials given by

$$L_n^a(x) = \frac{e^x x^{-a}}{n!} \frac{d^n}{dx^n} (e^{-x} x^{n+a}). \quad (31)$$

Then, both protocols still work in the case of homodyne detection with non-unit quantum efficiency, by using the noisy estimators in Eq. (29). Note that Eq. (29) imposes an efficiency $\eta > \frac{1}{2}$ for the estimator to be well-defined.

6 Verification protocols with heterodyne detection

6.1 Heterodyne detection

Heterodyne detection, also known as double homodyne, dual-homodyne, or eight-port homodyne detection [49], constitutes a single-mode Gaussian measurement that projects onto (unnormalized) coherent states. In mathematical terms, performing single-mode heterodyne detection on a state ρ involves sampling from the Husimi Q phase-space quasiprobability distribution [62]:

$$Q_\rho(\alpha) = \frac{1}{\pi} \langle \alpha | \rho | \alpha \rangle, \quad (32)$$

where $|\alpha\rangle = e^{-\frac{1}{2}|\alpha|^2} \sum_{n \geq 0} \frac{\alpha^n}{\sqrt{n!}} |n\rangle$ is the coherent state of amplitude $\alpha \in \mathbb{C}$. Experimentally, heterodyne measurement is implemented by mixing the state to be measured with vacuum through a beam splitter and doing a double homodyne detection, where the state to be measured is split into two using a beam splitter and two homodyne detections are implemented to measure perpendicular quadratures, with outcomes x and p , and get the complex number $\alpha = x + ip$ as the output.

On the other hand, an *unbalanced heterodyne measurement* is implemented by unbalancing the beam splitter splitting the state into two and changing the phase of the local oscillator, and allows the measurement of squeezed coherent states in phase space. Mathematically, the POVMs of unbalanced heterodyne detection over m modes

with unbalancing parameters $\boldsymbol{\xi} = \{\xi_1, \dots, \xi_m\} \in \mathbb{C}^m$ are given by

$$\Pi_{\boldsymbol{\alpha}}^{\boldsymbol{\xi}} = \frac{1}{\pi^m} |\boldsymbol{\alpha}, \boldsymbol{\xi}\rangle \langle \boldsymbol{\alpha}, \boldsymbol{\xi}|, \quad (33)$$

for all $\boldsymbol{\alpha} = \{\alpha_1, \dots, \alpha_m\} \in \mathbb{C}^m$. Here $|\boldsymbol{\alpha}, \boldsymbol{\xi}\rangle = \bigotimes_{i=1}^m |\alpha_i, \xi_i\rangle$ is a tensor product of squeezed coherent states $|\alpha_i, \xi_i\rangle$. Writing $\xi = r e^{i\theta}$, the unbalancing parameter is related to the optical setup by $r = \log\left(\frac{T}{R}\right)$, where T and R are the reflectance and transmittance of the unbalanced beam splitter, respectively, with the phase of the local oscillator being $-\frac{\theta}{2}$ [51].

6.2 k -mode heterodyne fidelity estimation

We now elaborate on how we can estimate the fidelity of a k -mode system using heterodyne detection, by generalizing heterodyne estimator functions from [51, 63].

Given an output experimental state ρ , the individual density matrix elements are given as

$$\rho_{mn} = \int_{\alpha \in \mathbb{C}} Q_\rho(\alpha) P_{mn}(\alpha) d\alpha, \quad (34)$$

where P_{mn} is the Glauber–Sudarshan P function of the operator $|n\rangle \langle m|$ and Q_ρ is the Husimi Q function of ρ . Since the Glauber–Sudarshan P function is often singular, we use a regularised version of the P function as our heterodyne estimator function. It is defined as

$$g_{mn}^{p(\text{het})}(\boldsymbol{\alpha}, \tau) = g_{m_1 n_1}^{p_1(\text{het})}(\alpha_1, \tau) \cdots g_{m_k n_k}^{p_k(\text{het})}(\alpha_k, \tau), \quad (35)$$

where $g_{mn}^{p(\text{het})}(\alpha, \tau)$ is given by

$$g_{m,n}^{p(\text{het})}(z, \tau) = \sum_{j=0}^{p-1} (-1)^j \tau^j f_{m+j, n+j}(z, \tau) \times \sqrt{\binom{m+j}{m} \binom{n+j}{n}}, \quad (36)$$

where for all k, l ,

$$f_{k,l}(z, \tau) := \frac{1}{\tau^{1+\frac{k+l}{2}}} e^{(1-\frac{1}{\tau})zz^*} \mathcal{L}_{l,k}\left(\frac{z}{\sqrt{\tau}}\right), \quad (37)$$

with

$$\begin{aligned} \mathcal{L}_{l,k}(z) &= e^{zz^*} \frac{(-1)^{k+l}}{\sqrt{k!l!}} \frac{\partial^{k+l}}{\partial z^k \partial z^{*l}} e^{-zz^*} \\ &= \sum_{p=0}^{\min(k,l)} \frac{\sqrt{k!l!} (-1)^p}{p!(k-p)!(l-p)!} z^{l-p} z^{*k-p} \end{aligned} \quad (38)$$

Here p_i and τ are free parameters, for $i \in \{1, \dots, k\}$.

Unlike the homodyne estimator functions from section 5, these regularised heterodyne estimators are no longer unbiased, however their bias can be controlled analytically:

Lemma 4 (Biased heterodyne estimators). *Let $k \in \mathbb{N}^*$, let $p_1, \dots, p_k \in \mathbb{N}^*$, let $m_1, n_1, \dots, m_k, n_k \in \mathbb{N}$, $\mathbf{m}, \mathbf{n} = \{m_1, n_1, \dots, m_k, n_k\}$ and let $0 < \tau \leq 1$. Let $\rho = \sum_{\mathbf{m}, \mathbf{n}=\mathbf{0}}^{\infty} \rho_{\mathbf{m}, \mathbf{n}} |\mathbf{m}\rangle\langle \mathbf{n}|$. Then,*

$$\left| \rho_{\mathbf{m}, \mathbf{n}} - \mathbb{E}_{\alpha \leftarrow Q_{\rho}} \left[g_{m_1 n_1}^{p_1(\text{het})}(\alpha_1, \tau) \dots g_{m_k n_k}^{p_k(\text{het})}(\alpha_k, \tau) \right] \right| \leq \epsilon^{\mathbf{P}}(k). \quad (40)$$

Here $\epsilon^{\mathbf{P}}(k)$ is a number independent of ρ which can be brought arbitrarily close to zero by tuning the free parameters, whose expressions is given in section F of the appendix.

We direct the reader to section F of the appendix for the proof.

Since sampling from the Husimi Q function corresponds to heterodyne detection, Lemma 4 allows us to estimate the individual elements of a k -mode density matrix using heterodyne detection by computing the mean of the function $\mathbf{z} \mapsto g_{\mathbf{m}\mathbf{n}}^{\mathbf{P}(\text{het})}(\mathbf{z}, \tau)$ over these samples, while controlling analytically the approximation error. The result generalises the bound obtained for the heterodyne estimator in [51] in the case $k = 1$. We can control the approximation error by controlling the value of the free parameters p_1, \dots, p_k, τ .

Therefore, given an experimental state ρ and target core state $|\mathbf{C}\rangle = \sum_{\mathbf{0} \leq \mathbf{n} \leq \mathbf{c}-1} c_{\mathbf{n}} |\mathbf{n}\rangle$ where $\mathbf{c} = \{c_1, \dots, c_k\} \in (\mathbb{N}^*)^k$, $\mathbf{n} = \{n_1, \dots, n_k\}$ and for all $\mathbf{p} = \{p_1, \dots, p_k\} \in (\mathbb{N}^*)^k$, and $0 < \tau \leq 1$, we define the function

$$g_{\mathbf{k}\text{-est}}^{(\text{het})}(\alpha, \tau, \mathbf{p}) = \sum_{\mathbf{0} \leq \mathbf{m}, \mathbf{n} \leq \mathbf{c}-1} c_{\mathbf{m}}^* c_{\mathbf{n}} g_{\mathbf{m}\mathbf{n}}^{\mathbf{p}}(\alpha, \tau), \quad (41)$$

for all $\alpha = \{\alpha_1, \dots, \alpha_k\} \in \mathbb{C}^k$. Computing the mean of $g_{\mathbf{k}\text{-est}}^{(\text{het})}(\alpha, \tau, \mathbf{p})$ over N heterodyne detections gives us an estimate of the fidelity between the experimental state and the target core state. Based on this, we describe a protocol for k -mode fidelity estimation using heterodyne

sampling, with the assumption that the different copies sent by the quantum device are i.i.d.:

Protocol 3. (*k -mode fidelity estimation using heterodyne detection*). *Let $c_1, \dots, c_k \in \mathbb{N}^*$ and let $|\mathbf{C}\rangle = \sum_{\mathbf{0} \leq \mathbf{n} \leq \mathbf{c}-1} c_{\mathbf{n}} |\mathbf{n}\rangle$ be a core state over k modes. Let also $N \in \mathbb{N}^*$ and $\mathbf{p} = \{p_1, \dots, p_k\} \in (\mathbb{N}^*)^k$ and let $0 < \tau < 1$ be free parameters. Let $\rho^{\otimes(N+1)}$ be $N+1$ copies of an unknown k -mode (mixed) quantum state ρ .*

1. *Measure N copies of ρ with homodyne detection, obtaining the samples $\alpha^{(1)}, \dots, \alpha^{(N)} \in \mathbb{R}^k$.*
2. *For $i \in \{1, \dots, k\}$ Compute the mean of the function $\alpha \mapsto g_{\mathbf{k}\text{-est}}^{(\text{het})}(\alpha, \tau, \mathbf{p})$ over the samples $\alpha^{(1)}, \dots, \alpha^{(N)} \in \mathbb{R}^k$*
3. *The mean gives an estimate of the fidelity $F_C^{(\mathbf{k}\text{-est})}(\tau)$.*

$F_C^{(\mathbf{k}\text{-est})}(\tau)$ gives an estimate of the fidelity between the remaining copy of ρ and the target state. The efficiency of the protocol is summarized by the following result:

Theorem 3 (Efficiency of Protocol 3). *Let $\lambda > 0$. With the notations of Protocol 3, it is possible to find N_1 such that for $N \geq N_1$, the estimate $F_C^{\mathbf{k}\text{-est}}(\tau)$ is ϵ -close to the real fidelity $F(\rho, |\mathbf{C}\rangle)$ with the probability $1 - \delta$, with ϵ and δ given by*

$$\epsilon = \lambda + \epsilon_{(\text{bias})}(\mathbf{C}, \mathbf{p}, \tau), \quad (42)$$

$$\delta = 2 \exp\left(-\frac{N\lambda^2}{2(R(\mathbf{C}, \mathbf{p}, \tau)^2)}\right), \quad (43)$$

where λ represents the statistical error, $\epsilon_{(\text{bias})}(\mathbf{C}, \mathbf{p}, \tau)$ represents the biased error of the estimator independent of ρ which can be made arbitrarily close to zero by tuning the free parameters \mathbf{p} and τ , and $R(\mathbf{C}, \mathbf{p}, \tau)$ represents the range of the estimator $g_{\mathbf{k}\text{-est}}^{(\text{het})}(\alpha, \tau, \mathbf{p})$. The expressions of $\epsilon_{(\text{bias})}(\mathbf{C}, \mathbf{p}, \tau)$ and $R(\mathbf{C}, \mathbf{p}, \tau)$ are given in section G of the appendix.

We direct the reader to section G of the appendix for the proof, which combines Lemma 4. Here λ represents the statistical error whereas $\epsilon_{(\text{bias})}(\mathbf{C}, \mathbf{p}, \tau)$ represents the estimator error. Therefore, after implementing protocol 3, the remaining copy of the state ρ is ϵ close to the target state with high probability. The value of the

free parameters \mathbf{p} and τ can be optimized according to the experiment, and obeying the constraint imposed by Eqs. (42) and (43) to minimize the number of measurements needed to be done to obtain the required precision. Note that the term $R(\mathbf{C}, \mathbf{p}, \tau)$ scales roughly as R^k , where R is the range of g_{mn} , therefore there is an exponential growth in the number of samples required to achieve a desired level of precision in terms of k (we prove this heuristically in section H of the appendix). This is expected as tomography generally scales exponentially in the number of modes.

We detail how to remove the i.i.d. assumption in section I of the appendix. The underlying idea is that with a limited number of samples, if we choose to measure certain samples while disregarding others, we can treat the overall state as permutation invariant. Note that the permutation applies to the multiple rounds of the verification protocol, i.e., involving multiple m -mode states. The essential takeaway from this proof is that removing the i.i.d. assumption produces an overhead in terms of the number of samples we need to take to certify the state (to see it from theorem 6, consider the extra error term, and the higher chance of the error not being bounded). While the protocol is efficient from a theoretical standpoint, combining this with the exponential overhead in the number of samples that comes from using a multimode fidelity estimator, the cost of removing the i.i.d. assumption becomes unrealistic in any near-term experimental scenario.

6.3 Robust multimode heterodyne verification

Suppose we are tasked to certify an m -mode quantum state ρ produced by an experiment, given N samples of such states. Combining the k -mode fidelity estimation protocol with the k -mode fidelity witness introduced in Eq. (12), together with the property of heterodyne measurements described in lemma 5, we can estimate the lower bound on the fidelity between any quantum state ρ and any target state of the form

$$\left(\bigotimes_{i=1}^m \hat{G}_i \right) \hat{U} \left(\bigotimes_{i=1}^{m/k} |C_i\rangle \right) = \hat{S}(\xi) \hat{D}(\beta) \hat{U} \left(\bigotimes_{i=1}^{m/k} |C_i\rangle \right) \quad (44)$$

where $|C_i\rangle$ is a k -mode core state and $i \in \{1, \dots, m/k\}$ are blocks of k -modes. Eq. (44)

forms the class of states which can be verified efficiently by our protocol. Under the assumption that k is a divisor of m , we obtain a protocol for multimode fidelity estimation using the k -mode fidelity estimate. But first, we state the lemma proved in [51], which highlights an important property of heterodyne detection.

Lemma 5 (Back-propagation of heterodyne measurement [51]). *Let $\beta, \xi \in \mathbb{C}^m$ and let $\hat{V} = \hat{S}(\xi) \hat{D}(\beta) \hat{U}$, where \hat{U} is an m -mode passive linear transformation with $m \times m$ unitary matrix U . For all $\gamma \in \mathbb{C}^m$, let $\alpha = U^\dagger(\gamma - \beta)$. Then,*

$$\Pi_\gamma^\xi = \hat{V} \Pi_\alpha^\xi \hat{V}^\dagger \quad (45)$$

where the expression for Π_γ^ξ is given by Eq. (33).

Similar to Lemma 2, a notable consequence is that the specific type of quantum operations \hat{V} in the lemma performed prior to a balanced heterodyne measurement can be effectively reversed by adjusting the heterodyne measurement to be appropriately unbalanced and then applying classical operations to the resulting samples. For instance, if we can certify $\bigotimes_{i=1}^{m/k} |C_i\rangle$ using balanced

heterodyne detection, we can certify $\hat{V} \bigotimes_{i=1}^{m/k} |C_i\rangle$ by unbalanced heterodyne detection and efficiently classical post-processing the samples obtained.

Now that we have prepared the necessary background, we can describe the protocol for multimode fidelity estimation using heterodyne detection under the i.i.d. assumption.

Protocol 4. (*Multimode fidelity witness with heterodyne detection estimation using k -mode fidelity witness*). *Let $c_1, \dots, c_m \in \mathbb{N}^*$. Let $|C_i\rangle = \sum_{n=0}^{c_i-1} c_{i,n} |n\rangle$ be a core state, for all $i \in \{1, \dots, m\}$. Let \hat{U} be an m -mode passive linear transformation with $m \times m$ unitary matrix U , and let $\beta, \xi \in \mathbb{C}^m$. We write $|\psi\rangle = \hat{S}(\xi) \hat{D}(\beta) \hat{U} \bigotimes_{i=1}^m |C_i\rangle$ as the m -mode target pure state. Let $N \in \mathbb{N}^*$ and let $p_1, \dots, p_m \in \mathbb{N}^*$ and $0 < \tau_1, \dots, \tau_{m/k} < 1$ be free parameters. Let $\rho^{\otimes N+1}$ be $N+1$ copies of an unknown m -mode (mixed) quantum state ρ .*

1. Measure all m subsystems of N copies of ρ with unbalanced heterodyne detection with unbalancing parameters $\xi = \{\xi_1, \dots, \xi_m\}$, obtaining the vectors of samples $\gamma^{(1)}, \dots, \gamma^{(N)} \in \mathbb{C}^m$.

2. For all $k \in \{1, \dots, N\}$, compute the vectors $\boldsymbol{\alpha}^{(k)} = U^\dagger(\boldsymbol{\gamma}^{(k)} - \boldsymbol{\beta})$. We write $\boldsymbol{\alpha}^{(k)} = (\alpha_1^{(k)}, \dots, \alpha_m^{(k)}) \in \mathbb{C}^m$
3. Partition the m modes into m/k blocks of k -mode states. For each of the blocks $i \in \{1, \dots, m/k\}$, calculate the mean $F_{C_i}^{(k-est)}(\tau_i)$ of the function $\mathbf{z} \mapsto g_{\text{het}_i}^{k-est}(\mathbf{z}, \tau_i, \mathbf{p}_i)$ (defined in Eq. (41), where \mathbf{p}_i is the vector containing the free parameters p for the k modes in the block), over the samples $\boldsymbol{\alpha}_i^{(1)}, \dots, \boldsymbol{\alpha}_i^{(N)} \in \mathbb{C}^k$.
4. Compute the fidelity witness estimate $W_\psi^{(k)} = 1 - \sum_{i=1}^{m/k} (1 - F_{C_i}^{(k-est)})$.

$W_\psi^{(k)}$ gives an estimate of the lower bound on the fidelity between unknown quantum state ρ and the target state $S(\boldsymbol{\xi})D(\boldsymbol{\beta})\hat{U} \left(\bigotimes_{i=1}^{m/k} |C_i\rangle \right)$. The efficiency of the protocol is summarized by the following theorem.

Theorem 4 (Efficiency of Protocol 4). *Let $\lambda_i > 0 \forall i \in \{1, \dots, m\}$. With the notations of Protocol 4, there exists N_2 such that for $N \geq N_2$, the estimate $W_\psi^{(k)}$ follows the bound*

$$1 - \frac{m}{k}(1 - F(\rho, |\psi\rangle)) - \epsilon \leq W_\psi^{(k)} \leq F(\rho, |\psi\rangle) + \epsilon \quad (46)$$

with probability $1 - \delta$. Here ϵ and δ are given by

$$\epsilon = \sum_{i=1}^{m/k} (\lambda_i + \epsilon_{(\text{bias})}(\mathbf{C}_i, \mathbf{p}_i, \tau_i)), \quad (47)$$

$$\delta = 2 \sum_{i=1}^{m/k} \exp\left(-\frac{N\lambda_i^2}{2(R(\mathbf{C}_i, \mathbf{p}_i, \tau_i))^2}\right), \quad (48)$$

where $\epsilon_{(\text{bias})}(\mathbf{C}_i, \mathbf{p}_i, \tau_i)$ and $R(\mathbf{C}_i, \mathbf{p}_i, \tau_i)$ represents the bias error and range of the estimator, as explained in Theorem 3. There are constants $K_1, K_2 > 0$ such that $N_2 = \tilde{\mathcal{O}}\left(\frac{K_1^k}{\epsilon^{2+k_2}} \log\left(\frac{1}{\delta}\right)\right)$, up to poly m factors.

We direct the reader to section J of the appendix for the proof. The free parameters $\boldsymbol{\tau} = \{\tau_1, \dots, \tau_{m/k}\}$ and $\mathbf{p} = \{p_1, \dots, p_m\}$ can be optimized with the constraints given by Eqs. (47) and (48) to obtain the minimal number of samples need to get the required precision with the required probability. Therefore, this protocol gives

us the method of certifying the quantum state produced by an experiment/quantum device, by grouping k modes together. Note that for $k = 1$, the certification can be done in polynomial time [51]. Whereas for any other k , the number of samples required to get a desired precision scale exponentially in k , but we get a tighter lower bound on the fidelity. Therefore, it becomes useful to recognize the cases where single-mode fidelities are close enough to the actual fidelity, and where it is useful to take $k > 1$, as discussed in section 4.2.

6.4 Verification of doped Gaussian states

Building on k -mode fidelity witness, this section details the protocol to verify a class of *doped Gaussian states*, which are non-Gaussian states recently introduced in [54] which can be prepared by applying Gaussian unitaries and at most t non-Gaussian κ -local unitaries on the vacuum state. However, since the classical post-processing does not apply to squeezing operations, we restrict our Gaussian unitaries to displacement operators and passive linear transformations. This is shown in figure 5. In particular, this protocol builds on the modified version of theorem 6 of [54], which we detail below:

Theorem 5. *(Non-Gaussianity compression in t -doped Gaussian unitaries and states). If $n \geq \kappa t$, any n -mode t -doped Gaussian unitary U with the Gaussian unitaries restricted to passive linear transformations and displacement operators can be decomposed as*

$$\hat{U} = \hat{G}(\hat{u}_{\kappa t} \otimes \mathbb{1}_{n-\kappa t})\hat{G}_{\text{passive}}, \quad (49)$$

for some suitable Gaussian unitary \hat{G} , energy-preserving Gaussian unitary \hat{G}_{passive} , and κt -mode (non-Gaussian) unitary $\hat{u}_{\kappa t}$. In particular, any n -mode t -doped Gaussian state can be decomposed as

$$|\psi\rangle = \hat{G}(|\phi_{\kappa t}\rangle \otimes |0\rangle^{(n-\kappa t)}) \quad (50)$$

for some suitable Gaussian unitary \hat{G} and κt -mode (non-Gaussian) state $|\phi_{\kappa t}\rangle$.

A visual representation of this theorem is given in the figure 5.

For the circuits where G is of the form $\hat{S}(\boldsymbol{\xi})\hat{D}(\boldsymbol{\beta})\hat{U}$ and $|\phi\rangle$ has a finite support size, efficient verification of such doped Gaussian states

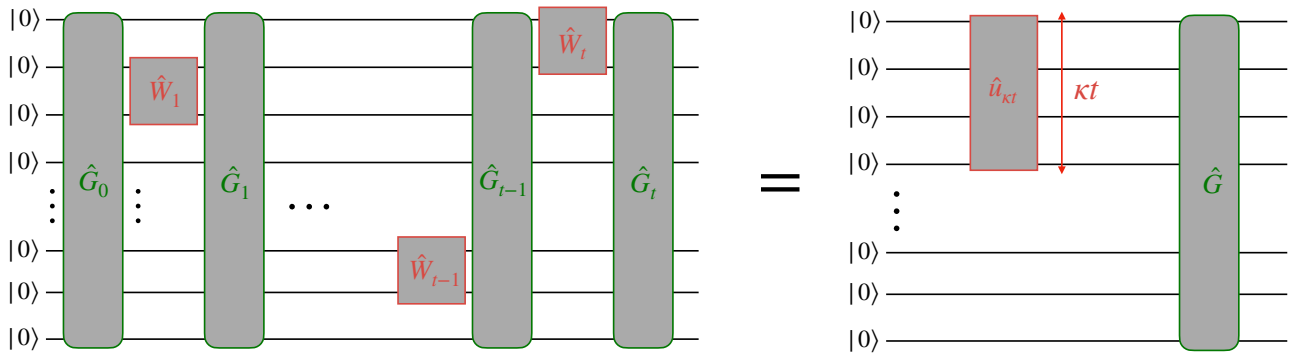


Figure 5: Pictorial representation of a t -doped Gaussian state from [54]. By definition, a t -doped Gaussian state vector $|\psi\rangle$ is prepared by applying Gaussian unitaries G_0, \dots, G_t (green boxes) and at most t non-Gaussian κ -local unitaries W_1, \dots, W_t (red boxes) to the n -mode vacuum. G_0, \dots, G_t are restricted to passive linear transformations and displacement operators for the classical post-processing to work. The figure also shows the decomposition proved in Theorem 5, which establishes that all the non-Gaussianity in $|\psi\rangle$ can be compressed in a localized region consisting of κt modes via a Gaussian unitary G .

is a direct application of Protocol 4 together with Theorem 5. The details of the protocol are given in section K of the appendix, where it is shown that verification is efficient for $\kappa t = O(\log m)$.

6.5 Imperfect heterodyne detection

Our heterodyne verification protocols have been described under the assumption of unit efficiency of the detector. For an arbitrary quantum efficiency η , we show in section L of the appendix that the single-mode heterodyne estimator $g_{m,n}^{p(\text{het})}$ and the Husimi Q function should be modified as:

$$g_{k,l}^{p(\text{het})}(z, \eta, \tau) := \sum_{j=0}^{p-1} (-1)^j f_{k+j, l+j}(z) t^j \times \sqrt{\binom{j+k}{k} \binom{j+l}{l}} \quad (51)$$

where $t = 1 - \eta + \tau\eta^2$, and $Q^\eta(\alpha) := \frac{1}{\eta} W(\frac{\alpha}{\sqrt{\eta}}, 1 - 2\eta^{-1})$ where for all $s < 0$,

$$W(\alpha, s) = -\frac{2}{1+s} \int_{\beta \in \mathbb{C}} Q(\beta) e^{\frac{2}{1+s} |\alpha - \beta|^2} \frac{d^2 \beta}{\pi}. \quad (52)$$

Then, heterodyne verification protocols still work in the case of heterodyne detection with non-unit quantum efficiency, by using the noisy estimator in Eq. (51) and smoothed Husimi Q function given by Eq. (52). Unlike noisy homodyne verification, the estimator functions are well-defined for all possible values of $\eta > 0$.

7 Comparing homodyne and heterodyne verification

After describing protocols for state verification using homodyne and heterodyne detection, we are in a position to compare these two Gaussian measurements in terms of their utility for state verification. For multimode state verification using witnesses based on single-mode fidelities, the protocol using homodyne sampling is more efficient for its verifiable states (unbiased estimators and quadratic polynomial dependence on ϵ for homodyne sampling protocol compared to biased estimators and a higher polynomial dependence for heterodyne sampling). However, undoing quantum operations in classical post-processing is only possible for orthogonal passive linear unitaries in homodyne sampling, as compared to the possibility of classical post-processing all passive linear unitaries with heterodyne sampling. Therefore, heterodyne sampling is applicable to a wider range of efficient verification scenarios as compared to homodyne sampling.

Furthermore, since classical post-processing with homodyne sampling requires all the modes to be measured at the same angle (which we referred to as parallel homodyne detection), the sampling over multiple modes is tomographically incomplete. Therefore, estimation of witnesses based on k -mode fidelities is only possible with parallel homodyne detection when $k = 1$, whereas, as illustrated in section 4, we can come

up with protocols utilizing fidelity witness with heterodyne sampling for state verification based on k -mode fidelities with $k > 1$. The use of such fidelity witnesses allows for the efficient verification of certain doped Gaussian states [54] using heterodyne sampling, while as far as we know it is not possible with homodyne sampling.

Finally, for noisy measurement devices with quantum efficiency η , noisy unbiased homodyne estimators are only well-defined for $\eta > 1/2$, whereas noisy biased heterodyne estimators are defined for all $\eta > 0$.

8 Conclusion

In this paper, we have introduced a general verification framework, which combines efficient and robust fidelity witnesses for tensor product target states, together with classical post-processing implementing measurement back-propagation. We have also introduced new families of such fidelity witnesses which outperform existing ones in terms of robustness, and identified both analytically and through numerical examples a trade-off between the sample complexity and the robustness of those witnesses.

To illustrate the applicability of our framework, we have focused on continuous-variable verification of multimode bosonic quantum states, using parallel homodyne detection as well as heterodyne detection. Our protocols are based on (ideal or lossy) homodyne and heterodyne estimators for the fidelity, and allow us to efficiently verify large classes of highly entangled and non-Gaussian continuous-variable quantum states such as doped Gaussian states, with rigorous confidence intervals.

Our protocols have been described under the i.i.d. assumption. This mimics an experimental situation, where different copies of the quantum state are reasonably independent of each other. Since we are mainly concerned with experimental situations, our i.i.d. assumption is justified. However, to make our protocols useful for quantum cryptography scenarios in which the quantum state to be verified is being prepared by a potential adversarial prover, one needs to derive a protocol without the i.i.d. assumption. We have sketched how to achieve this by modifying our Protocol 3 in section I of the appendix.

The certificates obtained through our verifi-

cation protocols are robust bounds on the fidelity. As such, they can be used for calibrating large quantum devices at the state preparation stage, but also for rigorously witnessing quantum properties of experimental states: by targeting a pure state with a desired quantum property, such as entanglement or non-Gaussianity, a sufficiently large fidelity provides a witness of that property [64, 65]. Furthermore, as fidelity provides a bound on total variation distance, these certificates can be used to support demonstrations of quantum computational speedups in an hardware-agnostic way, and serve as the basis for rigorous, hardware-agnostic quantum benchmarks of quantum computers.

As we have uncovered various applications of our verification framework in the continuous-variable setting, a natural follow-up is to investigate the applications to the efficient verification of discrete-variable quantum states. In this setting, other families of robust fidelity witnesses are readily available [36, 39] and could be combined with classical post-processing implementing measurement back-propagation to obtain efficient verification protocols of large classes of discrete-variable quantum states. We leave this to future work.

Acknowledgements

U.C. acknowledges inspiring discussions with A. Eriksson, S. Gasparinetti, G. Ferrini, A. Ferraro, G. Roeland, M. Walschaers, D. Hangleiter, H. Ollivier, F. A. Mele, and S. F. E. Oliviero. We acknowledge funding from the European Union’s Horizon Europe Framework Programme (EIC Pathfinder Challenge project Veriqub) under Grant Agreement No. 101114899.

References

- [1] J. Preskill, “Quantum computing and the entanglement frontier,” [arXiv:1203.5813 \[quant-ph\]](#).
- [2] T. F. Rønnow, Z. Wang, J. Job, S. Boixo, S. V. Isakov, D. Wecker, J. M. Martinis, D. A. Lidar, and M. Troyer, “Defining and detecting quantum speedup,” *Science* **345**, 420–424 (2014).
- [3] A. Harrow and A. Montanaro, “Quantum

- computational supremacy,” *Nature* **549**, 203–209 (2017).
- [4] P. W. Shor, “Algorithms for quantum computation: discrete logarithms and factoring,” in *Proceedings 35th annual symposium on foundations of computer science*, pp. 124–134, Ieee. 1994.
- [5] S. Aaronson and A. Arkhipov, “The computational Complexity of Linear Optics,” *Theory of Computing* **9**, 143 (2013), [arXiv:1011.3245](https://arxiv.org/abs/1011.3245).
- [6] B. M. Terhal and D. P. DiVincenzo, “Adaptive quantum computation, constant depth quantum circuits and Arthur-Merlin games,” *Quantum Information & Computation* **4**, 134–145 (2004), [arXiv:0205133](https://arxiv.org/abs/0205133).
- [7] D. Shepherd and M. J. Bremner, “Temporally unstructured quantum computation,” *Proceedings of the Royal Society A: Mathematical, Physical and Engineering Sciences* **465**, 1413–1439 (2009).
- [8] M. J. Bremner, R. Jozsa, and D. J. Shepherd, “Classical simulation of commuting quantum computations implies collapse of the polynomial hierarchy,” *Proceedings of the Royal Society A: Mathematical, Physical and Engineering Sciences* **467**, 459–472 (2011).
- [9] S. Boixo, S. V. Isakov, V. N. Smelyanskiy, R. Babbush, N. Ding, Z. Jiang, M. J. Bremner, J. M. Martinis, and H. Neven, “Characterizing quantum supremacy in near-term devices,” *Nature Physics* **14**, 595–600 (2018).
- [10] R. Mezher, J. Ghalbouni, J. Dgheim, and D. Markham, “Efficient approximate unitary t-designs from partially invertible universal sets and their application to quantum speedup,” [arXiv:1905.01504](https://arxiv.org/abs/1905.01504).
- [11] D. Hangleiter and J. Eisert, “Computational advantage of quantum random sampling,” *Reviews of Modern Physics* **95**, 035001 (2023).
- [12] F. Arute, K. Arya, R. Babbush, and et al., “Quantum supremacy using a programmable superconducting processor,” *Nature* **574**, 505–510 (2019).
- [13] H. S. Zhong, H. Wang, Y. H. Deng, M. C. Chen, L. C. Peng, Y. H. Luo, J. Qin, D. Wu, X. Ding, Y. Hu, et al., “Quantum computational advantage using photons,” *Science* **370**, 1460–1463 (2020).
- [14] L. S. Madsen, F. Laudenbach, M. F. Askarani, F. Rortais, T. Vincent, J. F. F. Bulmer, F. M. Miatto, L. Neuhaus, L. G. Helt, M. J. Collins, A. E. Lita, T. Gerrits, S. W. Nam, V. D. Vaidya, M. Menotti, I. Dhand, Z. Vernon, N. Quesada, and J. Lavoie, “Quantum computational advantage with a programmable photonic processor,” *Nature* **606**, 75–81 (2022).
- [15] T. Giordani, F. Flamini, M. Pompili, N. Viggianiello, N. Spagnolo, A. Crespi, R. Osellame, N. Wiebe, M. Walschaers, A. Buchleitner, and F. Sciarrino, “Experimental statistical signature of many-body quantum interference,” *Nature Photonics* **12**, 173–178 (2018).
- [16] H. Wang, J. Qin, X. Ding, M.-C. Chen, S. Chen, X. You, Y.-M. He, X. Jiang, L. You, Z. Wang, C. Schneider, J. J. Renema, S. Höfling, C.-Y. Lu, and J.-W. Pan, “Boson Sampling with 20 Input Photons and a 60-Mode Interferometer in a 10^{14} -Dimensional Hilbert Space,” *Phys. Rev. Lett.* **123**, 250503 (2019).
- [17] J. Preskill, “Lecture notes for a course on quantum computation,” 1998. <http://www.theory.caltech.edu/people/preskill/ph229>. Unpublished lecture notes.
- [18] E. Knill, “Quantum computing with realistically noisy devices,” *Nature* **434**, 39–44 (2005).
- [19] D. Leichtle, *Security and Efficiency of Delegated Quantum Computing*. Theses, Sorbonne Université, Feb., 2024. <https://theses.hal.science/tel-04718138>.
- [20] J. Eisert, D. Hangleiter, N. Walk, I. Roth, D. Markham, R. Parekh, U. Chabaud, and E. Kashefi, “Quantum certification and benchmarking,” *Nature Reviews Physics* **2**, 382–390 (2020).
- [21] G. M. D’Ariano, M. G. Paris, and M. F. Sacchi, “Quantum tomography,” *Advances in Imaging and Electron Physics* **128**, 206–309 (2003), [arXiv:quant-ph/0302028](https://arxiv.org/abs/quant-ph/0302028).
- [22] L. M. Artiles, R. D. Gill, and M. Gut̃a, “An invitation to quantum tomography,” *Journal of the Royal Statistical Society*

- Series B: Statistical Methodology* **67**, 109–134 (2005).
- [23] R. Renner, “Symmetry of large physical systems implies independence of subsystems,” *Nature Physics* **3**, 645–649 (2007).
- [24] A. Gheorghiu, T. Kapourniotis, and E. Kashefi, “Verification of quantum computation: An overview of existing approaches,” *Theory of Computing Systems* **4**, 715–808 (2019).
- [25] J. Eisert, D. Hangleiter, N. Walk, I. Roth, D. Markham, R. Parekh, U. Chabaud, and E. Kashefi, “Quantum certification and benchmarking,” *Nature Reviews Physics* **1–9** (2020).
- [26] A. Broadbent, J. Fitzsimons, and E. Kashefi, “Universal blind quantum computation,” in *2009 50th Annual IEEE Symposium on Foundations of Computer Science*, pp. 517–526, IEEE. 2009.
- [27] U. Mahadev, “Classical verification of quantum computations,” in *2018 IEEE 59th Annual Symposium on Foundations of Computer Science (FOCS)*, pp. 259–267, IEEE. 2018.
- [28] G. D. Kahanamoku-Meyer, “Forging quantum data: classically defeating an IQP-based quantum test,” *Quantum* **7**, 1107 (2023).
- [29] M.-H. Yung and B. Cheng, “Anti-Forging Quantum Data: Cryptographic Verification of Quantum Cloud Computing,” [arXiv:2005.01510 \[quant-ph\]](https://arxiv.org/abs/2005.01510).
- [30] Z. Brakerski, P. Christiano, U. Mahadev, U. Vazirani, and T. Vidick, “A cryptographic test of quantumness and certifiable randomness from a single quantum device,” in *2018 IEEE 59th Annual Symposium on Foundations of Computer Science (FOCS)*, pp. 320–331, IEEE. 2018.
- [31] Z. Brakerski, V. Koppula, U. Vazirani, and T. Vidick, “Simpler Proofs of Quantumness,” [arXiv:2005.04826 \[quant-ph\]](https://arxiv.org/abs/2005.04826).
- [32] N. Spagnolo, C. Vitelli, M. Bentivegna, D. J. Brod, A. Crespi, F. Flamini, S. Giacomini, G. Milani, R. Ramponi, P. Mataloni, *et al.*, “Experimental validation of photonic Boson Sampling,” *Nature Photonics* **8**, 615–620 (2014).
- [33] P. D. Drummond, B. Opanchuk, A. Delliou, and M. D. Reid, “Simulating complex networks in phase space: Gaussian boson sampling,” *Phys. Rev. A* **105**, 012427 (2022).
- [34] S. Aaronson and A. Arkhipov, “Boson Sampling is far from uniform,” [arXiv:1309.7460 \[quant-ph\]](https://arxiv.org/abs/1309.7460).
- [35] S. Ferracin, T. Kapourniotis, and A. Datta, “Accrediting outputs of noisy intermediate-scale quantum computing devices,” *New Journal of Physics* **21**, 113038 (2019).
- [36] D. Hangleiter, M. Kliesch, M. Schwarz, and J. Eisert, “Direct certification of a class of quantum simulations,” *Quantum Science and Technology* **2**, 015004 (2017).
- [37] M. Ringbauer, M. Hinsche, T. Feldker, P. K. Faehrmann, J. Bermejo-Vega, C. Edmunds, L. Postler, R. Stricker, C. D. Marciniak, M. Meth, *et al.*, “Verifiable measurement-based quantum random sampling with trapped ions,” [arXiv:2307.14424](https://arxiv.org/abs/2307.14424).
- [38] Z. Liu, D. Devulapalli, D. Hangleiter, Y.-K. Liu, A. J. Kollár, A. V. Gorshkov, and A. M. Childs, “Efficiently verifiable quantum advantage on near-term analog quantum simulators,” [arXiv:2403.08195](https://arxiv.org/abs/2403.08195).
- [39] H.-Y. Huang, J. Preskill, and M. Soleimanifar, “Certifying almost all quantum states with few single-qubit measurements,” [arXiv:2404.07281](https://arxiv.org/abs/2404.07281).
- [40] S. L. Braunstein and P. van Loock, “Quantum information with continuous variables,” *Rev. Mod. Phys.* **77**, 513–577 (2005).
- [41] C. Weedbrook, S. Pirandola, R. García-Patrón, N. J. Cerf, T. C. Ralph, J. H. Shapiro, and S. Lloyd, “Gaussian quantum information,” *Rev. Mod. Phys.* **84**, 621–669 (2012).
- [42] S. Yokoyama, R. Ukai, S. C. Armstrong, C. Sornphiphatphong, T. Kaji, S. Suzuki, J. ichi Yoshikawa, H. Yonezawa, N. C. Menicucci, and A. Furusawa, “Ultra-large-scale continuous-variable cluster states multiplexed in the time domain,” *Nature Photonics* **7**, 982 (2013).

- [43] D. Gottesman, A. Kitaev, and J. Preskill, “Encoding a qubit in an oscillator,” *Phys. Rev. A* **64**, 012310 (2001).
- [44] M. Mirrahimi, Z. Leghtas, V. V. Albert, S. Touzard, R. J. Schoelkopf, L. Jiang, and M. H. Devoret, “Dynamically protected cat-qubits: a new paradigm for universal quantum computation,” *New Journal of Physics* **16**, 045014 (2014).
- [45] M. H. Michael, M. Silveri, R. T. Brierley, V. V. Albert, J. Salmilehto, L. Jiang, and S. M. Girvin, “New Class of Quantum Error-Correcting Codes for a Bosonic Mode,” *Phys. Rev. X* **6**, 031006 (2016).
- [46] G. Adesso, S. Ragy, and A. R. Lee, “Continuous Variable Quantum Information: Gaussian States and Beyond,” *Open Systems & Information Dynamics* **21**, 1440001 (2014).
- [47] S. D. Bartlett, B. C. Sanders, S. L. Braunstein, and K. Nemoto, “Efficient Classical Simulation of Continuous Variable Quantum Information Processes,” *Physical Review Letters* **88**, 097904 (2002).
- [48] J.-I. Yoshiakawa, S. Yokoyama, T. Kaji, C. Sornphiphatphong, Y. Shiozawa, K. Makino, and A. Furusawa, “Invited article: Generation of one-million-mode continuous-variable cluster state by unlimited time-domain multiplexing,” *APL Photonics* **1**, 060801 (2016).
- [49] A. Ferraro, S. Olivares, and M. G. A. Paris, “Gaussian States in Quantum Information,” [arxiv:quant-ph/0503237](https://arxiv.org/abs/quant-ph/0503237).
- [50] L. Aolita, C. Gogolin, M. Kliesch, and J. Eisert, “Reliable quantum certification of photonic state preparations,” *Nature Communications* **6**, 8498 (2015).
- [51] U. Chabaud, F. Grosshans, E. Kashefi, and D. Markham, “Efficient verification of Boson Sampling,” *Quantum* **5**, 578 (2021).
- [52] Y.-C. Liu, J. Shang, and X. Zhang, “Efficient verification of entangled continuous-variable quantum states with local measurements,” *Phys. Rev. Res.* **3**, L042004 (2021).
- [53] Y.-D. Wu, G. Bai, G. Chiribella, and N. Liu, “Efficient verification of continuous-variable quantum states and devices without assuming identical and independent operations,” *Physical Review Letters* **126**, 240503 (2021).
- [54] F. A. Mele, A. A. Mele, L. Bittel, J. Eisert, V. Giovannetti, L. Lami, L. Leone, and S. F. Oliviero, “Learning quantum states of continuous variable systems,” [arXiv:2405.01431](https://arxiv.org/abs/2405.01431).
- [55] M. A. Nielsen and I. L. Chuang, “Quantum Computation and Quantum Information: 10th Anniversary Edition,” **Cambridge University Press**, New York, NY, USA, 2011.
- [56] C. A. Fuchs and J. V. D. Graaf, “Cryptographic distinguishability measures for quantum-mechanical states,” *IEEE Transactions on Information Theory* **45**, 1216–1227 (1999).
- [57] W. Hoeffding, “Probability inequalities for sums of bounded random variables,” *Journal of the American Statistical Association* **58**, 13–30 (1963).
- [58] U. Chabaud, D. Markham, and F. Grosshans, “Stellar representation of non-Gaussian quantum states,” *Physical Review Letters* **124**, 063605 (2020).
- [59] G. M. D’Ariano, M. G. Paris, and M. F. Sacchi, “Quantum tomography,” *Advances in imaging and electron physics* **128**, S1076–S1670 (2003).
- [60] S. Gandhari, V. V. Albert, T. Gerrits, J. M. Taylor, and M. J. Gullans, “Precision Bounds on Continuous-Variable State Tomography Using Classical Shadows,” *PRX Quantum* **5**, 010346 (2024).
- [61] R. Renner and J. I. Cirac, “de Finetti Representation Theorem for Infinite-Dimensional Quantum Systems and Applications to Quantum Cryptography,” *Phys. Rev. Lett.* **102**, 110504 (2009).
- [62] H. Yuen and J. Shapiro, “Optical communication with two-photon coherent states-Part III: Quantum measurements realizable with photoemissive detectors,” *IEEE Transactions on Information Theory* **26**, 78–92 (1980).
- [63] U. Chabaud, T. Douce, F. Grosshans, E. Kashefi, and D. Markham, “Building Trust for Continuous Variable Quantum States,” in *15th Conference on the Theory of Quantum Computation, Communication*

- and *Cryptography*. 2020.
[arXiv:1905.12700](#).
- [64] O. Gühne and G. Tóth, “Entanglement detection,” *Physics Reports* **474**, 1–75 (2009).
- [65] U. Chabaud, G. Roeland, M. Walschaers, F. Grosshans, V. Parigi, D. Markham, and N. Treps, “Certification of Non-Gaussian States with Operational Measurements,” *PRX Quantum* **2**, 020333 (2021).
- [66] I. Sen, “Physical interpretation of non-normalizable harmonic oscillator states and relaxation to pilot-wave equilibrium,” *Scientific Reports* **14**, 669 (2024).
- [67] J.-M. Aubry, C. Butucea, and K. Meziani, “State estimation in quantum homodyne tomography with noisy data,” *Inverse Problems* **25**, 015003 (2008).
- [68] Arvind, B. Dutta, N. Mukunda, and R. Simon, “The real symplectic groups in quantum mechanics and optics,” *Pramana* **45**, 471–497 (1995).
- [69] A. Leverrier, R. García-Patrón, R. Renner, and N. J. Cerf, “Security of Continuous-Variable Quantum Key Distribution Against General Attacks,” *Phys. Rev. Lett.* **110**, 030502 (2013).
- [70] M. G. Paris, “Quantum state measurement by realistic heterodyne detection,” *Physical Review A* **53**, 2658 (1996).
- [71] A. Wünsche, “Laguerre 2D-functions and their application in quantum optics,” *Journal of Physics A: Mathematical and General* **31**, 8267 (1998).
- [72] J. Peřina and L. Miřta, ““Regular” form of the Sudarshan-Glauber representation of the density matrix,” *Physics Letters A* **27**, 217–218 (1968).
- [73] H. W. Gould, “Combinatorial Identities: A standardized set of tables listing 500 binomial coefficient summations,” Morgantown, W Va, 1972.

Appendix

A Robust fidelity witnesses: Proof of Lemma 2

We start by the proof of Eq. (13) in Lemma 2. The proof breaks down the m -mode system into blocks of k modes and combines the known inequality in each of the blocks to obtain the final inequality.

Let's consider a k -mode system with the density matrix $\rho_{1\dots k} = \text{Tr}_{\{1,\dots,m\}\setminus\{1,\dots,k\}}[\rho]$ and target state $|\psi_1\rangle \otimes \dots \otimes |\psi_k\rangle$. For this k -mode state,

$$W^{(k)}(\rho, \psi) = 1 - (1 - F(\rho_{1,\dots,k}, |\psi_1\rangle \otimes \dots \otimes |\psi_k\rangle)) = F(\rho_{1,\dots,k}, |\psi_1\rangle \otimes \dots \otimes |\psi_k\rangle). \quad (53)$$

Using Eq. (23)

$$W^{(1)}(\rho_{1\dots k}, |\psi_1\rangle \otimes \dots \otimes |\psi_k\rangle) \leq W^{(k)}(\rho_{1\dots k}, |\psi_1\rangle \otimes \dots \otimes |\psi_k\rangle), \quad (54)$$

$$1 - \sum_{i=1}^k (1 - F(\rho_i, |\psi_i\rangle)) \leq 1 - (1 - F(\rho_{1\dots k}, |\psi_1\rangle \otimes \dots \otimes |\psi_k\rangle)), \quad (55)$$

$$\sum_{i=1}^k (1 - F(\rho_i, |\psi_i\rangle)) \geq (1 - F(\rho_{1\dots k}, |\psi_1\rangle \otimes \dots \otimes |\psi_k\rangle)). \quad (56)$$

Similarly,

$$\sum_{i=k+1}^{2k} (1 - F(\rho_i, |\psi_i\rangle)) \geq (1 - F(\rho_{k+1\dots 2k}, |\psi_{k+1}\rangle \otimes \dots \otimes |\psi_{2k}\rangle)), \quad (57)$$

$$\vdots \quad (58)$$

$$\sum_{i=m-(k-1)}^m (1 - F(\rho_i, |\psi_i\rangle)) \geq (1 - F(\rho_{m-(k-1)\dots m}, |\psi_{m-(k-1)}\rangle \otimes \dots \otimes |\psi_m\rangle)). \quad (59)$$

Summing over,

$$\sum_{i=1}^m (1 - F(\rho_i, |\psi_i\rangle)) \geq \sum_{i=1}^{m/k} (1 - F(\rho_{ki-(k-1)\dots ki}, |\psi_{ki-(k-1)}\rangle \otimes \dots \otimes |\psi_{ki}\rangle)), \quad (60)$$

$$1 - \sum_{i=1}^m (1 - F(\rho_i, |\psi_i\rangle)) \leq 1 - \sum_{i=1}^{m/k} (1 - F(\rho_{ki-(k-1)\dots ki}, |\psi_{ki-(k-1)}\rangle \otimes \dots \otimes |\psi_{ki}\rangle)), \quad (61)$$

$$W^{(1)}(\rho, \psi) \leq W^{(k)}(\rho, \psi). \quad (62)$$

We now turn to the proof of Eq. (14) in Lemma 2. This proof relies on relating the fidelity between two states to the fidelity between two corresponding substates of the given states.

The fidelity between two states ρ and $|\psi\rangle = |\psi_1\rangle \otimes \dots \otimes |\psi_m\rangle$ is given by

$$F(\rho, |\psi_1\rangle \otimes \dots \otimes |\psi_m\rangle) = \text{Tr}[\rho |\psi_1\rangle \langle \psi_1| \otimes \dots \otimes |\psi_m\rangle \langle \psi_m|] \quad (63)$$

$$\leq \text{Tr}[\rho \mathbb{1} \otimes \dots \otimes |\psi_{ki-(k-1)}\rangle \langle \psi_{ki-(k-1)}| \otimes \dots \otimes |\psi_{ki}\rangle \langle \psi_{ki}| \otimes \dots \otimes \mathbb{1}] \quad (64)$$

$$= F(\rho_{ki-(k-1)\dots ki}, |\psi_{ki-(k-1)}\rangle \otimes \dots \otimes |\psi_{ki}\rangle). \quad (65)$$

Therefore,

$$\frac{m}{k} F(\rho, |\psi\rangle) \leq \sum_{i=1}^{m/k} F(\rho_{ki-(k-1)\dots ki}, |\psi_{ki-(k-1)}\rangle \otimes \dots \otimes |\psi_{ki}\rangle), \quad (66)$$

$$1 - \frac{m}{k} + \frac{m}{k} F(\rho, |\psi\rangle) \leq 1 - \frac{m}{k} + \sum_{i=1}^{m/k} F(\rho_{ki-(k-1)\dots ki}, |\psi_{ki-(k-1)}\rangle \otimes \dots \otimes |\psi_{ki}\rangle), \quad (67)$$

$$1 - \frac{m}{k} (1 - F(\rho, |\psi\rangle)) \leq W^{(k)}(\rho, \psi). \quad (68)$$

Also

$$F(\boldsymbol{\rho}, |\boldsymbol{\psi}\rangle) = \text{Tr}[\boldsymbol{\rho} |\psi_1\rangle \langle \psi_1| \otimes \cdots \otimes |\psi_m\rangle \langle \psi_m|] \quad (69)$$

$$= \text{Tr}[\boldsymbol{\rho} \mathbb{1}] - \text{Tr}[\boldsymbol{\rho} (\mathbb{1} - |\psi_1\rangle \langle \psi_1| \otimes \cdots \otimes |\psi_k\rangle \langle \psi_k|) \otimes I] \quad (70)$$

$$- \text{Tr}[\boldsymbol{\rho} |\psi_1\rangle \langle \psi_1| \otimes \cdots \otimes |\psi_k\rangle \langle \psi_k| \otimes (1 - |\psi_{k+1}\rangle \langle \psi_{k+1}| \otimes \cdots \otimes |\psi_{2k}\rangle \langle \psi_{2k}|) \otimes I] \quad (71)$$

$$\vdots \quad (72)$$

$$- \text{Tr}[\boldsymbol{\rho} |\psi_1\rangle \langle \psi_1| \otimes \cdots \otimes |\psi_{m-k}\rangle \langle \psi_{m-k}| \otimes (1 - |\psi_{m-(k-1)}\rangle \langle \psi_{m-(k-1)}| \otimes \cdots \otimes |\psi_m\rangle \langle \psi_m|)] \quad (73)$$

$$\geq 1 - \sum_{i=1}^{m/k} \text{Tr}[\boldsymbol{\rho} \mathbb{1} \otimes (\mathbb{1} - |\psi_{ki-(k-1)}\rangle \langle \psi_{ki-(k-1)}| \otimes \cdots \otimes |\psi_{ki}\rangle \langle \psi_{ki}|) \otimes \mathbb{1}] \quad (74)$$

$$= 1 - \sum_{i=1}^{m/k} \left(1 - F(\boldsymbol{\rho}_{ki-(k-1)\dots ki}, |\psi_{ki-(k-1)}\rangle \otimes \cdots \otimes |\psi_{ki}\rangle)\right) = W^{(k)}(\boldsymbol{\rho}, \boldsymbol{\psi}). \quad (75)$$

B Normalizable and unnormalizable eigenfunctions of the harmonic oscillator

For an eigenvalue j of the harmonic oscillator, let $K = 2j + 1$. We define the functions

$$h_0^K(x) := 1 + \sum_{n=1}^{\infty} \frac{\prod_{i=0}^{n-1} (4i + 1 - K)}{(2n)!} x^{2n}, \quad (76)$$

$$h_1^K(x) := x + \sum_{n=1}^{\infty} \frac{\prod_{i=0}^{n-1} (4i + 3 - K)}{(2n + 1)!} x^{2n+1}. \quad (77)$$

Then, the normalizable eigenfunctions of the harmonic oscillator are given by [66]:

$$\psi_j^{(\text{nor})}(x) = \begin{cases} N_j e^{-x^2/2} h_0^K(x), & \text{if } j \text{ is even,} \\ N_j e^{-x^2/2} h_1^K(x), & \text{if } j \text{ is odd,} \end{cases} \quad (78)$$

where N_j is a normalization constant. Similarly, the unnormalizable eigenfunctions are given by

$$\psi_j^{(\text{unnor})}(x) = \begin{cases} e^{-x^2/2} h_1^K(x), & \text{if } j \text{ is even,} \\ e^{-x^2/2} h_0^K(x), & \text{if } j \text{ is odd.} \end{cases} \quad (79)$$

C Efficiency of homodyne single-mode fidelity estimation: Proof of Theorem 1

The proof of Theorem 1 combines Eq. (19) with Hoeffding's statistical sampling inequality (Lemma 1) to estimate the statistical error in calculating the mean of $g_C^{(\text{hom})}$ with a finite number of samples.

If $(x^{(1)}, \theta^{(1)}), \dots, (x^{(N)}, \theta^{(N)}) \in \mathbb{R}^2$ are the samples obtained by homodyne detection, then

$$F_C = \frac{1}{N} \sum_{i=1}^N g_C^{(\text{hom})}(x^{(i)}, \theta^{(i)}). \quad (80)$$

Also, if ρ_{kl} are the elements of the density matrix ρ in the fock basis, then the actual fidelity between ρ and $|C\rangle$

$$F(\rho, |C\rangle) = \sum_{k,l=0}^{c-1} c_k^* c_l \rho_{kl} = \sum_{k,l=0}^{c-1} c_k^* c_l \mathbb{E}_{P_{\rho \rightarrow (x,\theta)}} [f_{lk}(x) e^{i(l-k)\theta}]. \quad (81)$$

From Eq. (19). Therefore,

$$F_C = \sum_{k,l=0}^{c-1} c_k^* c_l \frac{1}{N} \sum_{i=1}^N (f_{lk}(x^{(i)}) e^{i(l-k)\theta^{(i)}}), \quad (82)$$

$$|F(\rho, |C\rangle) - F_C| = \left| \sum_{k,l=0}^{c-1} c_k^* c_l \left(\mathbb{E}_{P_{\rho \rightarrow (x,\theta)}} [f_{lk}(x) e^{i(l-k)\theta}] - \frac{1}{N} \sum_{i=1}^N (f_{lk}(x^{(i)}) e^{i(l-k)\theta^{(i)}}) \right) \right|. \quad (83)$$

Using Hoeffding's inequality,

$$\Pr [|F(\rho, |C\rangle) - F_C| \geq \lambda] \leq 2 \exp \left[-\frac{2N\lambda^2}{G^2} \right], \quad (84)$$

where $G = \max(g_C^{\text{hom}}(x, \theta)) - \min(g_C^{\text{hom}}(x, \theta))$.

$$|g_C^{\text{hom}}(x, \theta)| = \left| \sum_{k,l=0}^{c-1} c_k^* c_l f_{lk}(x) e^{i(l-k)\theta} \right| \leq \sum_{k,l=0}^{c-1} |c_k^* c_l f_{lk}(x) e^{i(l-k)\theta}| \leq \sum_{k,l=0}^{c-1} |f_{lk}(x) e^{i(l-k)\theta}|. \quad (85)$$

Using Lemma 1 in [67],

$$|g_C^{\text{hom}}(x, \theta)| \leq K_\infty C^{\frac{10}{3}}, \quad (86)$$

where C is the support size of the core state and K_∞ is a constant. Therefore, $G \leq 2K_\infty C^{\frac{10}{3}}$, and

$$\Pr [|F(\rho, |C\rangle) - F_C| \geq \lambda] \leq 2 \exp \left[-\frac{N\lambda^2}{2(K_\infty C^{10/3})^2} \right]. \quad (87)$$

Therefore, for a given error ϵ ,

$$|F(\rho, |C\rangle) - F_C| \leq \epsilon, \quad (88)$$

with the probability $1 - \delta$, where $\delta = 2 \exp \left[-\frac{N\epsilon^2}{2(K_\infty C^{10/3})^2} \right]$. For fixed ϵ and δ , therefore, $|F_C^{\text{est}}(\rho) - F_C^{\text{real}}| \leq \epsilon$, for $N \geq N_1$, where

$$N_1 = \mathcal{O} \left(\left(\frac{C^{\frac{10}{3}}}{\epsilon} \right)^2 \log \left(\frac{1}{\delta} \right) \right). \quad (89)$$

D Back-propagation of parallel homodyne measurement: Proof of Lemma 3

The proof of Lemma 3 uses the effect of a unitary on the quadrature operators to determine the properties the unitary should have for the transformed state to be an eigenstate of the non-rotated quadrature operators.

The action of \hat{O} on the quadrature operators can be described as

$$\hat{O} \begin{bmatrix} \hat{X}^{(1)} \\ \hat{X}^{(2)} \\ \vdots \\ \hat{P}^{(1)} \\ \vdots \\ \hat{P}^{(m)} \end{bmatrix} \hat{O}^\dagger = S_O \begin{bmatrix} \hat{X}^{(1)} \\ \hat{X}^{(2)} \\ \vdots \\ \hat{P}^{(1)} \\ \vdots \\ \hat{P}^{(m)} \end{bmatrix}. \quad (90)$$

Where S_O is a $2m \times 2m$ unitary matrix. Therefore,

$$\hat{X}^{(1)} \hat{O} |\mathbf{x}\rangle = \hat{O} \left(S_O \begin{bmatrix} \hat{X}^{(1)} \\ \hat{X}^{(2)} \\ \vdots \\ \hat{P}^{(1)} \\ \vdots \\ \hat{P}^{(m)} \end{bmatrix} \right)_1 |\mathbf{x}\rangle. \quad (91)$$

If S_O is a block diagonal matrix with two $m \times m$ blocks, i.e. if S_O can be expressed as

$$S_O = \begin{bmatrix} (S_O)_1 & \mathbf{0} \\ \mathbf{0} & (S_O)_2 \end{bmatrix}, \quad (92)$$

where $(S_O)_1$ and $(S_O)_2$ are $m \times m$ matrices. Then

$$\left(S_O \begin{bmatrix} \hat{X}^{(1)} \\ \hat{X}^{(2)} \\ \vdots \\ \hat{P}^{(1)} \\ \vdots \\ \hat{P}^{(m)} \end{bmatrix} \right)_1 = \left((S_O)_1 \begin{bmatrix} \hat{X}^{(1)} \\ \hat{X}^{(2)} \\ \vdots \\ \hat{X}^{(m)} \end{bmatrix} \right)_1. \quad (93)$$

And

$$\hat{X}^{(1)} \hat{O} |\mathbf{x}\rangle = ((S_O)_1 \mathbf{x})_1 \hat{O} |\mathbf{x}\rangle, \quad (94)$$

where \mathbf{x} is the vector of eigenvalues of $|\mathbf{x}\rangle$. Therefore $\hat{O} |\mathbf{x}\rangle_\theta$ is an eigenvector of \hat{X} with eigenvalue $(S_O)_1 \mathbf{x}_\theta$.

$$\hat{O} |\mathbf{x}\rangle = |(S_O)_1 \mathbf{x}\rangle. \quad (95)$$

Furthermore, it can be proven [68] that if S_O is block diagonal, it must be orthogonal, therefore $(S_O)_1$ and $(S_O)_2$ are orthogonal matrices. Now suppose that we rotate all the m -modes by an angle θ . So

$$\hat{X}_\theta^{(i)} = \hat{X}^{(i)} \cos \theta + \hat{P}^{(i)} \sin \theta, \quad (96)$$

$\forall i \in \{1, \dots, m\}$. After the application of \hat{O} , the quadratures transform as

$$\begin{bmatrix} \hat{X}_\theta^{(1)} \\ \hat{X}_\theta^{(2)} \\ \vdots \\ \hat{X}_\theta^{(m)} \end{bmatrix} = (S_O)_1 \begin{bmatrix} \hat{X}^{(1)} \\ \hat{X}^{(2)} \\ \vdots \\ \hat{X}^{(m)} \end{bmatrix} \cos \theta + (S_O)_2 \begin{bmatrix} \hat{P}^{(1)} \\ \hat{P}^{(2)} \\ \vdots \\ \hat{P}^{(m)} \end{bmatrix} \sin \theta. \quad (97)$$

If $(S_O)_1 = (S_O)_2$, then

$$\begin{bmatrix} \hat{X}_\theta^{(1)} \\ \hat{X}_\theta^{(2)} \\ \vdots \\ \hat{X}_\theta^{(m)} \end{bmatrix} = (S_O)_1 \begin{bmatrix} \hat{X}^{(1)} \cos \theta + \hat{P}^{(1)} \sin \theta \\ \hat{X}^{(2)} \cos \theta + \hat{P}^{(2)} \sin \theta \\ \vdots \\ \hat{X}^{(m)} \cos \theta + \hat{P}^{(m)} \sin \theta \end{bmatrix} = (S_O)_1 \begin{bmatrix} \hat{X}_\theta^{(1)} \\ \hat{X}_\theta^{(2)} \\ \vdots \\ \hat{X}_\theta^{(m)} \end{bmatrix}. \quad (98)$$

Therefore,

$$\left(S_O \begin{bmatrix} \hat{X}_\theta^{(1)} \\ \hat{X}_\theta^{(2)} \\ \vdots \\ \hat{X}_{\theta+\pi/2}^{(1)} \\ \vdots \\ \hat{X}_{\theta+\pi/2}^{(m)} \end{bmatrix} \right)_1 = \left((S_O)_1 \begin{bmatrix} \hat{X}_\theta^{(1)} \\ \hat{X}_\theta^{(2)} \\ \vdots \\ \hat{X}_\theta^{(m)} \end{bmatrix} \right)_1. \quad (99)$$

And finally,

$$\hat{O} |\mathbf{x}\rangle_\theta = |(S_O)_1 \mathbf{x}\rangle_\theta. \quad (100)$$

Therefore, Eq. (100) only holds when S_O is a block diagonal matrix with two $m \times m$ blocks, and the two blocks being equal $(S_O)_1 = (S_O)_2$. Furthermore, if all the modes are not rotated by the same angle, then Eq. (100) does not hold.

Next,

$$\hat{D}(\boldsymbol{\beta}) |\mathbf{x}\rangle_\theta = |\mathbf{x} + \boldsymbol{\beta}_\theta\rangle_\theta, \quad (101)$$

where $\boldsymbol{\beta}_\theta$ is the component of $\boldsymbol{\beta}$ along θ . Finally,

$$\hat{V} \Pi_{\mathbf{x}_\theta} \hat{V}^\dagger = \hat{V} |\mathbf{x}\rangle_\theta \langle \mathbf{x}|_\theta \hat{V}^\dagger = \hat{D}(\boldsymbol{\beta}) \hat{O} |\mathbf{x}\rangle_\theta \langle \mathbf{x}|_\theta \hat{O}^\dagger \hat{D}(\boldsymbol{\beta})^\dagger, \quad (102)$$

$$\hat{V} \Pi_{\mathbf{x}_\theta} \hat{V}^\dagger = \hat{D}(\boldsymbol{\beta}) |(S_O)_1 \mathbf{x}\rangle_\theta \langle (S_O)_1 \mathbf{x}|_\theta \hat{D}(\boldsymbol{\beta})^\dagger = |(S_O)_1 \mathbf{x} + \boldsymbol{\beta}_\theta\rangle_\theta \langle (S_O)_1 \mathbf{x} + \boldsymbol{\beta}_\theta|_\theta. \quad (103)$$

Let $\mathbf{x}' = (S_O)_1 \mathbf{x} + \boldsymbol{\beta}_\theta$. Then,

$$\hat{V} \Pi_{\mathbf{x}_\theta} \hat{V}^\dagger = |\mathbf{x}'\rangle_\theta \langle \mathbf{x}'|_\theta = \Pi_{\mathbf{x}'_\theta}. \quad (104)$$

E Efficiency of homodyne verification: Proof of Theorem 2

The proof of Theorem 2 uses single-mode fidelity estimation with classical post-processing and statistical sampling inequality.

We first consider the case where $\hat{D}(\boldsymbol{\beta}) \hat{O} = \mathbb{1}$ and the target state is $|\psi\rangle = \bigotimes_{i=1}^m |C_i\rangle$, where $|C_i\rangle = \sum_{n=0}^{c_i-1} c_{i,n} |n\rangle$. If $\boldsymbol{\rho}_i$ is the reduced state of $\boldsymbol{\rho}$ in the i^{th} mode, then from Theorem 1

$$|F(\boldsymbol{\rho}_i, |C_i\rangle) - F_{C_i}| \leq \frac{\epsilon}{m}, \quad (105)$$

with probability greater than $1 - \delta_i$, where $\delta_i = 2 \exp\left[-\frac{N\epsilon^2}{2m^2(C_i^{10/3})^2}\right]$. Therefore, taking the union bound on probabilities,

$$\left| W_\psi - \sum_{i=1}^m (1 - F(\boldsymbol{\rho}_i, |C_i\rangle)) \right| = \left| \sum_{i=1}^m (F(\boldsymbol{\rho}_i, |C_i\rangle) - F_{C_i}) \right| \quad (106)$$

$$\leq \sum_{i=1}^m |F(\boldsymbol{\rho}_i, |C_i\rangle) - F_{C_i}| \quad (107)$$

$$\leq \epsilon. \quad (108)$$

with probability $1 - P_W^{i.i.d.}$, where

$$P_W^{i.i.d.} = 2 \sum_{i=1}^m \exp\left(-\frac{N\epsilon^2}{m^2(C_i^{10/3})^2}\right), \quad (109)$$

where C_i is the support size for the core state in the mode i . Combining this result with lemma 2,

$$1 - m(1 - F(\boldsymbol{\rho}, |\boldsymbol{\psi}\rangle)) - \epsilon \leq W_\psi \leq F(\boldsymbol{\rho}, |\boldsymbol{\psi}\rangle) + \epsilon, \quad (110)$$

with probability $1 - P_W^{i.i.d.}$, where $P_W^{i.i.d.}$ is given by Eq. (109). If $C := \max_{i \in \{1, \dots, m\}} c_i$, $\delta \leq (P_W^{i.i.d.})_{\max}$, where

$$(P_W^{i.i.d.})_{\max} = 2m \exp\left(-\frac{N\epsilon^2}{m^2(K_\infty C^{\frac{10}{3}})^2}\right). \quad (111)$$

So, for a given precision ϵ and probability $1 - \delta$, Eq. (110) is satisfied when $N \geq N_2$, with N_2 given by Eq. (28). We now generalize the proof to the case where the target state is of the form

$$|\boldsymbol{\psi}\rangle = \hat{D}(\boldsymbol{\beta}) \hat{O} \bigotimes_{i=1}^m |C_i\rangle, \quad (112)$$

where for all $i \in \{1, \dots, m\}$, $|C_i\rangle = \sum_{n=0}^{c_i-1} c_{i,n} |n\rangle$ is a core state, \hat{O} is an m -mode passive linear transformation with $2m \times 2m$ block diagonal orthogonal matrix S_O , and $\boldsymbol{\beta} \in \mathbb{C}^m$. Next, writing $\hat{V} := \hat{D}(\boldsymbol{\beta}) \hat{O}$ we make use of lemma 3 to write

$$\text{Tr}(\hat{V}^\dagger \boldsymbol{\rho} \hat{V} \Pi_{\mathbf{x}_\theta}) = \text{Tr}(\boldsymbol{\rho} \hat{V} \Pi_{\mathbf{x}_\theta} \hat{V}^\dagger) = \text{Tr}(\boldsymbol{\rho} \Pi_{(S_O \mathbf{x}_\theta + \boldsymbol{\beta})}). \quad (113)$$

In essence, by homodyne sampling, and classical post-processing $\mathbf{x}_\theta = S_O^{-1}(\mathbf{x}'_\theta - \boldsymbol{\beta})$, we can estimate the lower bound on the fidelity between $\hat{V}^\dagger \boldsymbol{\rho} \hat{V}$ and $\bigotimes_{i=1}^m |C_i\rangle$:

$$1 - m(1 - F(\hat{V}^\dagger \boldsymbol{\rho} \hat{V}, \bigotimes_{i=1}^m |C_i\rangle \langle C_i|)) - \epsilon \leq W_\psi \leq F(\hat{V}^\dagger \boldsymbol{\rho} \hat{V}, \bigotimes_{i=1}^m |C_i\rangle \langle C_i|) + \epsilon, \quad (114)$$

with probability greater than $1 - (P_W^{i.i.d.})_{\max}$, where $(P_W^{i.i.d.})_{\max}$ is given by Eq. (111). Given that

$$F(\hat{V}^\dagger \boldsymbol{\rho} \hat{V}, \bigotimes_{i=1}^m |C_i\rangle \langle C_i|) = F(\boldsymbol{\rho}, |\boldsymbol{\psi}\rangle). \quad (115)$$

We conclude

$$1 - m(1 - F(\boldsymbol{\rho}, |\boldsymbol{\psi}\rangle)) - \epsilon \leq W_\psi \leq F(\boldsymbol{\rho}, |\boldsymbol{\psi}\rangle) + \epsilon, \quad (116)$$

with probability greater than $1 - (P_W^{i.i.d.})_{\max}$, where $(P_W^{i.i.d.})_{\max}$ is given by Eq. (111).

F Controlling the bias of heterodyne multimode fidelity estimators: Proof of Lemma 4

Given an operator $\rho = \sum_{0 \leq k, l \leq c-1} \rho_{kl} |k\rangle \langle l|$ (we use the notation ρ since we are generally considering density matrices, but what follows also holds for operators which are not necessarily density matrices), it can be proven that [51]

$$E_{\alpha \leftarrow Q_\rho}[g_{m,n}^{(p)}(\alpha, \tau)] = \rho_{mn} + (-1)^{p+1} \sum_{q=p}^{\infty} \rho_{m+q, n+q} \tau^q \binom{q-1}{p-1} \sqrt{\binom{m+q}{m} \binom{n+q}{n}}. \quad (117)$$

Therefore, we have the expression for the bias error in a single-mode estimator. Using this result, we want to find the bias error when we multiply k of these estimators for the multimode heterodyne estimator. Defining

$$\Pi_{mn}^{(p)} := \int g_{m,n}^{(p)}(\alpha) Q_\rho(\alpha) d\alpha |\alpha\rangle \langle \alpha|, \quad (118)$$

Eq. (117) can be reinterpreted as

$$\Pi_{mn}^{(p)} = |m\rangle \langle n| + (-1)^{p+1} \sum_{q=p}^{\infty} |m\rangle \langle n| \tau^q \binom{q-1}{p-1} \sqrt{\binom{m+q}{m} \binom{n+q}{n}}. \quad (119)$$

We define

$$\Pi_{m,n,p}^{\text{err}} := (-1)^{p+1} \sum_{q=p}^{\infty} |m\rangle \langle n| \tau^q \binom{q-1}{p-1} \sqrt{\binom{m+q}{m} \binom{n+q}{n}}. \quad (120)$$

Let us first consider $k = 2$.

$$\mathbb{E}_{\alpha \leftarrow Q_{\rho}(\alpha)} [g_{m_1, n_1}^{(p_1)} g_{m_2, n_2}^{(p_2)}] = \text{Tr} \left[\Pi_{m_1 n_1}^{(p_1)} \otimes \Pi_{m_2 n_2}^{(p_2)} \rho \right] = \text{Tr} \left[(|m_1\rangle \langle n_1| + \Pi_{m_1, n_1, p_1}^{\text{err}}) \otimes (|m_2\rangle \langle n_2| + \Pi_{m_2, n_2, p_2}^{\text{err}}) \rho \right] \quad (121)$$

$$= \rho_{\frac{m_1 n_1}{m_2 n_2}} + \text{Tr} \left[|m_1\rangle \langle n_1| \otimes \Pi_{m_2, n_2, p_2}^{\text{err}} \rho \right] + \text{Tr} \left[\Pi_{m_1, n_1, p_1}^{\text{err}} \otimes |m_2\rangle \langle n_2| \rho \right] + \text{Tr} \left[\Pi_{m_1, n_1, p_1}^{\text{err}} \otimes \Pi_{m_2, n_2, p_2}^{\text{err}} \rho \right]. \quad (122)$$

Therefore,

$$\left| \rho_{\frac{m_1 n_1}{m_2 n_2}} - \mathbb{E}_{\alpha \leftarrow Q_{\rho}(\alpha)} [g_{m_1, n_1}^{(p_1)} g_{m_2, n_2}^{(p_2)}] \right| = \left| \text{Tr} \left[|m_1\rangle \langle n_1| \otimes \Pi_{m_2, n_2, p_2}^{\text{err}} \rho \right] \right| + \left| \text{Tr} \left[\Pi_{m_1, n_1, p_1}^{\text{err}} \otimes |m_2\rangle \langle n_2| \rho \right] \right| \quad (123)$$

$$+ \left| \text{Tr} \left[\Pi_{m_1, n_1, p_1}^{\text{err}} \otimes \Pi_{m_2, n_2, p_2}^{\text{err}} \rho \right] \right|. \quad (124)$$

Now,

$$\left| \text{Tr} \left[|m_1\rangle \langle n_1| \otimes \Pi_{m_2, n_2, p_2}^{\text{err}} \rho \right] \right| \leq \left\| |m_1\rangle \langle n_1| \otimes \Pi_{m_2, n_2, p_2}^{\text{err}} \right\|_{\text{HS}} \|\rho\|_{\text{HS}}, \quad (125)$$

where $\|\cdot\|_{\text{HS}}$ refers to the Hilbert-Schmidt norm.

$$\|\rho\|_{\text{HS}} = \sqrt{\text{Tr}[\rho^2]} \leq 1, \quad (126)$$

$$\left\| |m_1\rangle \langle n_1| \otimes \Pi_{m_2, n_2, p_2}^{\text{err}} \right\|_{\text{HS}} \leq \sqrt{\text{Tr}_1[|m_1\rangle \langle m_1|] \text{Tr}_2[(\Pi_{m_2, n_2, p_2}^{\text{err}})^\dagger \Pi_{m_2, n_2, p_2}^{\text{err}}]}. \quad (127)$$

Now,

$$\text{Tr}_2[(\Pi_{m_2, n_2, p_2}^{\text{err}})^\dagger \Pi_{m_2, n_2, p_2}^{\text{err}}] = \sqrt{\sum_{q_2=p_2}^{\infty} \tau^{2q_2} \binom{m_2+q_2}{m_2} \binom{n_2+q_2}{n_2}}. \quad (128)$$

Further,

$$\sum_{q_2=p_2}^{\infty} \tau^{2q_2} \binom{m_2+q_2}{m_2} \binom{n_2+q_2}{n_2} = \tau^{2p_2} \sum_{q_2=0}^{\infty} \tau^{2q_2} \binom{m_2+q_2+p_2}{m_2} \binom{n_2+q_2+p_2}{n_2}. \quad (129)$$

Using,

$$\binom{m_p+q}{m} \leq (1+m)^{p+q}, \quad (130)$$

$$\sum_{q_2=p_2}^{\infty} \tau^{2q_2} \binom{m_2+q_2}{m_2} \binom{n_2+q_2}{n_2} \leq \tau^{2p_2} (1+m_2)^{p_2} (1+n_2)^{p_2} \sum_{q_2=0}^{\infty} (\tau^2 (1+m_2)(1+n_2))^{q_2}. \quad (131)$$

If

$$\tau \leq \frac{1}{\sqrt{(1+m_2)(1+n_2)}}. \quad (132)$$

Then

$$\sum_{q_2=p_2}^{\infty} \tau^{2q_2} \binom{m_2+q_2}{m_2} \binom{n_2+q_2}{n_2} \leq \frac{\tau^{2p_2} (1+m_2)^{p_2} (1+n_2)^{p_2}}{1 - \tau^2 (1+m_2)(1+n_2)}. \quad (133)$$

Using this result in Eq. (123),

$$\left| \rho_{\substack{m_1 n_1 \\ m_2 n_2}} - \mathbb{E}_{\alpha \leftarrow Q_\rho(\alpha)} [g_{m_1, n_1}^{(p_1)} g_{m_2, n_2}^{(p_2)}] \right| \leq \frac{\tau^{p_2} (1+m_2)^{p_2/2} (1+n_2)^{p_2/2}}{\sqrt{1-\tau^2} (1+m_2)(1+n_2)} + \frac{\tau^{p_1} (1+m_1)^{p_1/2} (1+n_1)^{p_1/2}}{\sqrt{1-\tau^2} (1+m_1)(1+n_1)} \quad (134)$$

$$+ \frac{\tau^{p_1} (1+m_1)^{p_1/2} (1+n_1)^{p_1/2}}{\sqrt{1-\tau^2} (1+m_1)(1+n_1)} \times \frac{\tau^{p_2} (1+m_2)^{p_2/2} (1+n_2)^{p_2/2}}{\sqrt{1-\tau^2} (1+m_2)(1+n_2)}. \quad (135)$$

Calling

$$E_{m_1, n_1}^{p_1} := \frac{\tau^{p_1} (1+m_1)^{p_1/2} (1+n_1)^{p_1/2}}{\sqrt{1-\tau^2} (1+m_1)(1+n_1)}, \quad (136)$$

$$\left| \rho_{\substack{m_1 n_1 \\ m_2 n_2}} - \mathbb{E}_{\alpha \leftarrow Q_\rho(\alpha)} [g_{m_1, n_1}^{(p_1)} g_{m_2, n_2}^{(p_2)}] \right| \leq E_{m_1, n_1}^{p_1} + E_{m_2, n_2}^{p_2} + E_{m_1, n_1}^{p_1} E_{m_2, n_2}^{p_2} =: \epsilon^{(p_1, p_2)}(2). \quad (137)$$

By taking $\tau \rightarrow 0$, we can make $E_{m_1, n_1}^{p_1}$ and hence $\epsilon^{(p_1, p_2)}(2)$ arbitrarily close to zero.

By induction, it can be similarly proven that

$$\left| \rho_{\mathbf{m}, \mathbf{n}} - \mathbb{E}_{\alpha \leftarrow Q_\rho} [g_{m_1, n_1}^{(p_1)}(\alpha_1, \tau) \cdots g_{m_k, n_k}^{(p_k)}(\alpha_k, \tau)] \right| \leq E_{m_1, n_1}^{p_1} \epsilon^{(p_2, \dots, p_{k-1})}(k-1) + \epsilon^{(p_2, \dots, p_{k-1})}(k-1) + E_{m_1, n_1}^{p_1}. \quad (138)$$

Similar to the two-mode case, $\epsilon^{\mathbf{P}}(k)$ can be made to go to 0 by taking $\tau \rightarrow 0$.

G Efficiency of heterodyne multimode fidelity estimation: Proof of Theorem 3

The proof of Theorem 3 combines Lemma 4 with Hoeffding inequality (Lemma 1) to determine the maximum possible error in fidelity estimation.

The true fidelity between the mixed m -mode state ρ and the target state $|C\rangle = \sum_{\mathbf{0} \leq \mathbf{m}, \mathbf{n} \leq \mathbf{c}-1} c_{\mathbf{n}} |\mathbf{n}\rangle$ is given by

$$F_C(\rho) = \sum_{\mathbf{0} \leq \mathbf{m}, \mathbf{n} \leq \mathbf{c}-1} c_{\mathbf{m}}^* c_{\mathbf{n}} \rho_{\mathbf{m}\mathbf{n}}. \quad (139)$$

Let us denote

$$\mathbb{E}_{\alpha_1 \leftarrow Q_\rho(\alpha_1, \tau)} [g_{m_1, n_1}^{(p_1)}(\alpha_1, \tau)] \cdots \mathbb{E}_{\alpha_k \leftarrow Q_\rho(\alpha_k, \tau)} [g_{m_k, n_k}^{(p_k)}(\alpha_k, \tau)] = \mathbb{E}_{\alpha \leftarrow Q_\rho} [g_{\mathbf{m}\mathbf{n}}^{(\mathbf{p})}(\alpha, \tau)]. \quad (140)$$

Therefore,

$$F_C(\rho) - \mathbb{E}_{\alpha \leftarrow Q_\rho} \left[\sum_{\mathbf{0} \leq \mathbf{m}, \mathbf{n} \leq \mathbf{c}-1} c_{\mathbf{m}}^* c_{\mathbf{n}} g_{\mathbf{m}\mathbf{n}}^{(\mathbf{p})}(\alpha, \tau) \right] = \sum_{\mathbf{0} \leq \mathbf{m}, \mathbf{n} \leq \mathbf{c}-1} c_{\mathbf{m}}^* c_{\mathbf{n}} \left(\rho_{\mathbf{m}\mathbf{n}} - \mathbb{E}_{\alpha \leftarrow Q_\rho} [g_{\mathbf{m}\mathbf{n}}^{(\mathbf{p})}(\alpha, \tau)] \right). \quad (141)$$

From Lemma 4, $\left| \rho_{\mathbf{m}\mathbf{n}} - \mathbb{E}_{\alpha \leftarrow Q_\rho} [g_{\mathbf{m}\mathbf{n}}^{(\mathbf{p})}(\alpha, \tau)] \right| \leq \epsilon^{\mathbf{P}}(k)$. Therefore,

$$|F_C(\rho) - F_C^{\text{k-est}}(\rho, \tau)| \leq \sum_{\mathbf{0} \leq \mathbf{m}, \mathbf{n} \leq \mathbf{c}-1} |c_{\mathbf{m}}^* c_{\mathbf{n}}| \epsilon^{\mathbf{P}}(k) = \epsilon_{(\text{bias})}(\mathbf{C}, \mathbf{p}, \tau), \quad (142)$$

where

$$F_C^{\text{k-est}}(\rho, \tau) = \sum_{\mathbf{0} \leq \mathbf{m}, \mathbf{n} \leq \mathbf{c}-1} \frac{1}{N} \sum_{l=1}^N c_{\mathbf{m}}^* c_{\mathbf{n}} g_{\mathbf{m}\mathbf{n}}^{(\mathbf{p})}(\alpha^{(l)}, \tau). \quad (143)$$

Using Hoeffding's inequality,

$$\Pr \left[\left| \sum_{\mathbf{0} \leq \mathbf{m}, \mathbf{n} \leq \mathbf{c}-1} c_{\mathbf{m}}^* c_{\mathbf{n}} \left(\mathbb{E}_{\alpha \leftarrow Q_\rho} [g_{\mathbf{m}\mathbf{n}}^{(\mathbf{p})}(\alpha, \tau)] - \frac{1}{N} \sum_{l=1}^N (g_{\mathbf{m}\mathbf{n}}^{(\mathbf{p})}(\alpha^{(l)}, \tau)) \right) \right| \geq \lambda \right] = 2 \exp \left(-\frac{2N\lambda^2}{R^2} \right), \quad (144)$$

where $R = \max(\sum_{0 \leq m, n \leq c-1} c_m^* c_n g_{mn}^p) - \min(\sum_{0 \leq m, n \leq c-1} c_m^* c_n g_{mn}^p)$.

$$\begin{aligned} \left| \sum_{0 \leq m, n \leq c-1} c_m^* c_n g_{mn}^p \right| &\leq \sum_{0 \leq m, n \leq c-1} |c_m^* c_n| |g_{mn}^p| \\ &\leq \sum_{0 \leq m, n \leq c-1} |c_m^* c_n| \frac{1}{\tau^{1+\frac{m+n}{2}}} \binom{\max(m, n) + p}{p-1} \sqrt{2^{|m-n|} \binom{\max(m, n)}{\min(m, n)}} = R(\mathbf{C}, \mathbf{p}, \tau). \end{aligned} \quad (145)$$

And, $R \leq 2R(\mathbf{C}, \mathbf{p}, \tau)$. Therefore,

$$\Pr \left[\left| \sum_{0 \leq m, n \leq c-1} c_m^* c_n \left(\mathbb{E}_{\alpha \leftarrow Q_\rho} [g_{mn}^{(p)}(\alpha, \tau)] - \frac{1}{N} \sum_{l=1}^N (g_{mn}^p(\alpha^{(l)}, \tau)) \right) \right| \geq \lambda \right] \leq 2 \exp \left(-\frac{N\lambda^2}{2(R(\mathbf{C}, \mathbf{p}, \tau))^2} \right). \quad (146)$$

And

$$\begin{aligned} |F_C(\rho) - F_C^{\text{k-est}}(\tau)| &= \left| \sum_{0 \leq m, n \leq c-1} c_m^* c_n \left(\rho_{mn} - \frac{1}{N} \sum_{l=1}^N (g_{mn}^p(\alpha^{(l)}, \tau)) \right) \right| \\ &\leq \left| \sum_{0 \leq m, n \leq c-1} c_m^* c_n \left(\rho_{mn} - \mathbb{E}_{\alpha \leftarrow Q_\rho} [g_{mn}^{(p)}(\alpha, \tau)] \right) \right| \end{aligned} \quad (147)$$

$$+ \left| \sum_{0 \leq m, n \leq c-1} c_m^* c_n \left(\mathbb{E}_{\alpha \leftarrow Q_\rho} [g_{mn}^{(p)}(\alpha, \tau)] - \frac{1}{N} \sum_{l=1}^N (g_{mn}^p(\alpha^{(l)}, \tau)) \right) \right|. \quad (148)$$

$$\therefore |F_C(\rho) - F_C^{\text{k-est}}(\tau)| \leq \lambda + \epsilon_{(\text{bias})}(\mathbf{C}, \mathbf{p}, \tau). \quad (149)$$

$$\therefore |F_C(\rho) - F_C^{\text{k-est}}(\tau)| \leq \epsilon. \quad (150)$$

with probability $1 - \delta$, where $\delta = 2 \exp \left(-\frac{N\lambda^2}{2(R(\mathbf{C}, \mathbf{p}, \tau))^2} \right)$.

H Detailed study of the complexity in Theorem 3

Given

$$\epsilon = \lambda + \epsilon_{(\text{bias})}(\mathbf{C}, \mathbf{p}, \tau), \quad (151)$$

and

$$\delta = 2 \exp \left(-\frac{N\lambda^2}{2(R(\mathbf{C}, \mathbf{p}, \tau))^2} \right). \quad (152)$$

We want to find out that given ϵ and δ , how does the number of samples N scales with the number of modes that are grouped together, k . We can see from the expression for ϵ and δ that in general the scaling will be a complicated function depending on a lot of parameters. To make things easier and focus only on the scaling with k , we drop the dependence of $\epsilon^p(k)$, g_{mn}^p and $\epsilon_{(\text{bias})}(\mathbf{C}, \mathbf{p}, \tau)$ on $\mathbf{m}, \mathbf{n}, \mathbf{p}$. Therefore,

$$\epsilon_{(\text{bias})}(\mathbf{C}, \tau) = \sum_{0 \leq m, n \leq c-1} |c_m^* c_n| \epsilon(k) = \mathbf{c}^2 \epsilon(k). \quad (153)$$

Further, we call $E_{m_1, n_1}^{p_1}$ from Eq. (136) as $\epsilon(1)$.

$$\epsilon(k) = \epsilon(1)\epsilon(k-1) + \epsilon(1) + \epsilon(k-1). \quad (154)$$

We can further break down $\epsilon(k-1)$ as $\epsilon(k-1) = \epsilon(k-2)(\epsilon(1) + 1) + \epsilon(1)$ and so on. Therefore,

$$\epsilon(k) = \epsilon(1) \sum_{i=0}^{k-1} (\epsilon(1) + 1)^i. \quad (155)$$

Now,

$$\epsilon(1) = \frac{\tau^p(1+m)^{p/2}(1+n)^{p/2}}{\sqrt{1-\tau^2(1+m)(1+n)}}. \quad (156)$$

For $\tau^2 \leq \frac{1}{(1+m)(1+n)}$, $\epsilon(1) \ll 1$ and

$$\epsilon(k) \approx k\epsilon(1), \quad (157)$$

and

$$\epsilon(\text{bias})(\mathbf{C}, \tau) = \mathcal{O}(k\epsilon(1)). \quad (158)$$

Therefore,

$$\epsilon \approx \lambda + k\epsilon(1). \quad (159)$$

We have

$$\delta = 2 \exp\left(-\frac{N\lambda^2}{2 * (R(\mathbf{C}, \mathbf{p}, \tau))^2}\right) = 2 \exp\left(-\frac{N(\epsilon - k\epsilon(1))^2}{2 * (R(\mathbf{C}, \mathbf{p}, \tau))^2}\right). \quad (160)$$

Now,

$$\epsilon(1) = \frac{\tau^p(1+m)^{p/2}(1+n)^{p/2}}{\sqrt{1-\tau^2(1+m)(1+n)}}. \quad (161)$$

Assuming τ is very small. Therefore,

$$\epsilon' := k\epsilon(1) = \tau^p K_{mnk}(p), \quad (162)$$

where

$$K_{mnk}(p) := k \frac{(1+m)^{p/2}(1+n)^{p/2}}{\sqrt{1-\tau^2(1+m)(1+n)}}, \quad (163)$$

adjusting τ , we can make ϵ' as small possible, in particular we can make $\epsilon' = \epsilon/2$. If

$$\epsilon' = \tau^p K_{mnk}(p) \approx \epsilon, \quad (164)$$

$$\tau \approx \epsilon^{\frac{1}{p}} \frac{1}{(K_{mnk}(p))^{\frac{1}{p}}}. \quad (165)$$

Now,

$$R(\mathbf{C}, \mathbf{p}, \tau) = \sum_{0 \leq m, n \leq c-1} c_m^* c_n \frac{1}{\tau^{1+\frac{m+n}{2}}} \binom{\max(\mathbf{m}, \mathbf{n}) + \mathbf{p}}{\mathbf{p} - 1} \sqrt{2^{|\mathbf{m}-\mathbf{n}|} \binom{\max(\mathbf{m}, \mathbf{n})}{\min(\mathbf{m}, \mathbf{n})}}. \quad (166)$$

Asymptotically, it scales as

$$R(\mathbf{C}, \mathbf{p}, \tau) \approx \mathcal{O}\left(\frac{R^k}{\tau^{kc}}\right) = \mathcal{O}\left(\frac{R^k (K_{mnk}(p))^{\frac{kc}{p}}}{\epsilon^{\frac{kc}{p}}}\right). \quad (167)$$

Finally, the number of samples scale as

$$N = \mathcal{O}\left(\frac{R(\mathbf{C}, \mathbf{p}, \tau)^2}{\lambda^2} \log\left(\frac{1}{\delta}\right)\right) = \mathcal{O}\left(\frac{(R^2 (K_{mnk}(p))^{\frac{2c}{p}})^k}{\epsilon^{2+\frac{2kc}{p}}} \log\left(\frac{1}{\delta}\right)\right). \quad (168)$$

Therefore, the number of samples N scales exponentially with the number of modes. For $k = 1$, we recover the polynomial scaling derived in [51].

I Removing the i.i.d. assumption

In this section, we sketch how to remove the i.i.d. assumption in Protocol 3 by modifying it as follows:

Protocol 5. (*General t -mode fidelity estimation with heterodyne detection*) Let $|C\rangle = \sum_{\mathbf{0} \leq \mathbf{n} \leq \mathbf{c}-1} c_{\mathbf{n}} |\mathbf{n}\rangle$ be a core state, where $c_1, \dots, c_t \in \mathbb{N}^*$. Let also $N \in \mathbb{N}^*$, and let $p_1, \dots, p_t \in \mathbb{N}^*$, $E, S \in \mathbb{N}$ and $0 < \tau < 1$ be free parameters. Let ρ^{N+1} be an unknown t -mode quantum state over $N+1$ subsystems. We write $N = N' + K + 4Q$, for $N', K, Q \in \mathbb{N}$.

1. Measure $N = N' + K + 4Q$ subsystems of ρ^{N+1} chosen at random with heterodyne detection, obtaining the samples $\alpha_1, \dots, \alpha_{N'}, \beta_1, \dots, \beta_K, \gamma_1, \dots, \gamma_{4Q} \in \mathbb{C}^t$. Let ρ be the remaining state.
2. Discard the $4Q$ samples $\gamma_1, \dots, \gamma_{4Q}$.
3. Record the number R of samples β_i such that $\beta_i^\dagger \cdot \beta_i + 1 > E$, for $i = 1, \dots, K$. The protocol aborts if $R \geq S$.
4. Otherwise, compute the mean $F_C^{k\text{-est}}(\rho)$ of the function $\mathbf{z} \mapsto g_C^{k\text{-est}}(\mathbf{z}, \tau)$ (defined in Eq. 41) over the samples $\alpha_1, \dots, \alpha_{N'} \in \mathbb{C}^t$.
5. This gives the fidelity estimate $F_C^{k\text{-est}}$.

Note that this protocol differs from Protocol 3 due to the inclusion of two additional classical post-processing steps, specifically steps 2 and 3. These steps are integral to a de Finetti reduction for infinite-dimensional systems as detailed in [61]. Notably, step 3 involves an energy test, where the energy parameters E and S must be selected to ensure completeness. This means that if the perfect core state is sent, it will pass the energy test with high probability.

The value $F_C^{k\text{-est}}(\tau)$ obtained is an estimate of the fidelity between the remaining state ρ and the target core state $|C\rangle$. The efficiency of the protocol is summarised by the following result:

Theorem 6. Let $\epsilon > 0$. With the notations of Protocol 5,

$$\left| F_C(\rho) - F_C^{k\text{-est}}(\tau) \right| \leq \epsilon + A_C^{\mathbf{p}}(\tau) + P_{\text{deFinetti}}^C, \quad (169)$$

or the protocol aborts in step 3, with probability greater than $1 - (P_{\text{support}}^C + P_{\text{deFinetti}}^C + P_{\text{choice}}^C + P_{\text{Hoeffding}}^C)$, where

$$P_{\text{support}}^C = 8K^{3/2} \exp \left[-\frac{K}{9} \left(\frac{Q}{N'+1+4Q} - \frac{2S}{K} \right)^2 \right], \quad (170)$$

$$P_{\text{deFinetti}}^C = Q^{\frac{(E+1)^{2t}}{2}} \exp \left[-\frac{2Q(Q+1)}{N'+1+4Q} \right], \quad (171)$$

$$P_{\text{choice}}^C = \frac{4Q}{N'+1}, \quad (172)$$

$$P_{\text{Hoeffding}}^C = 2 \binom{N'+1}{4Q} \exp \left(-\frac{N'+1-4Q}{2} \left(\frac{\epsilon}{R(\mathbf{C}, \mathbf{p}, \tau)} - 8Q \right)^2 \right). \quad (173)$$

Proof. The proof follows these three steps:

- **Support estimation:** with probability arbitrarily close to 1, most of the subsystems of the permutation-invariant state $\rho^{N'+4Q}$ lie in a lower dimensional subspace, or the score of the state $\rho^{N'+4Q+K}$ at the support estimation step is high

- **De Finetti reduction:** any permutation-invariant state with most of its subsystems in a lower dimensional subspace admits a purification in the symmetric subspace that still has most of its subsystems in a lower dimensional subspace. This purification is well approximated by a mixture of almost-i.i.d. states;
- **Hoeffding inequality for almost-i.i.d. states:** mixture of almost-i.i.d. states can be certified in a similar fashion as i.i.d. states.

1.1 Support estimation for permutation invariant states

The proof essentially follows the proof in section E.1 in the appendix of [63], where Eq. (124) in the paper is modified using the following lemma [69]

Lemma 6. *Let T_n and U_n be defined as*

$$T_t := \frac{1}{\pi^t} \int_{\sum_{i=1}^t |\alpha_i|^2 \geq E} |\alpha_1\rangle \langle \alpha_1| \cdots |\alpha_t\rangle \langle \alpha_t| d\alpha_1 \cdots d\alpha_t,$$

and

$$U_t := \sum_{m=E+1}^{\infty} \Pi_m^t \text{ with } \Pi_m^t = \sum_{m_1+\cdots+m_t=m} |m_1 \cdots m_t\rangle \langle m_1 \cdots m_t|.$$

Then, the following inequality holds:

$$U_t \leq 2T_t.$$

Following the proof in section E.1 of [63], with $U \mapsto U_t, T \mapsto T_t, n \mapsto N' + 4Q + 1, s \mapsto S, q \mapsto Q$ and $k \mapsto K, \rho^{N'+4Q+1}$ will be successfully projected into

$$S_{\bar{\mathcal{H}}^{\otimes N'+1+4Q-Q}}^{N'+1+4Q} := \text{span} \bigcup_{\pi} \pi(\bar{\mathcal{H}}^{\otimes N'+1+3Q} \otimes \mathcal{H}^{\otimes Q}) \pi^{-1}, \quad (174)$$

or the protocol aborts ($R \geq S$) with probability P_{support}^C , given by Eq. (170). Note that

$$\bar{\mathcal{H}} = \bar{\mathcal{H}}_1 \otimes \cdots \otimes \bar{\mathcal{H}}_t, \quad (175)$$

$$\mathcal{H} = \mathcal{H}_1 \otimes \cdots \otimes \mathcal{H}_t, \quad (176)$$

where $\bar{\mathcal{H}}_i$ is a single mode Hilbert space of at most E photons, of dimension $E + 1 \forall i \in \{1, \dots, t\}$

1.2 De Finetti reduction

We modify Lemma 9 and Theorem 5 from [63] as follows

Lemma 7. *Any permutation-invariant state $\rho^{N'+1+4Q} \in S_{\bar{\mathcal{H}}^{\otimes N'+1+4Q-Q}}^{N'+1+4Q}$ has a purification $\tilde{\rho}^{N'+1+4Q}$ in $\text{Sym}^{N'+1+4Q}(\mathcal{H} \otimes \mathcal{H}) \cap S_{(\bar{\mathcal{H}} \otimes \bar{\mathcal{H}})^{\otimes N'+1+4Q-2Q}}^n$.*

where $\text{Sym}^n(\mathcal{K}) = \{\phi \in \mathcal{K}^{\otimes n}, \pi\phi = \phi (\forall \pi)\}$ and \mathcal{H} and $\bar{\mathcal{H}}$ are defined in Eq. (176). Here π refers to a permutation of subsystems.

For all $n, r \geq 0$ and all $|v\rangle \in \bar{\mathcal{H}} \otimes \bar{\mathcal{H}}$, the set of *almost-i.i.d. states along $|v\rangle$* , $S_{v^{\otimes n-r}}^n$, is defined as the span of all vectors that are, up to reorderings, of the form $|v\rangle^{\otimes n-r} \otimes |\phi\rangle$, for an arbitrary $|\phi\rangle \in (\mathcal{H} \otimes \mathcal{H})^{\otimes r}$. In the following, we simply refer to these states as *almost-i.i.d. states* (which becomes relevant when $r \ll n$).

Theorem 7. Let $\tilde{\rho}^{N'+1+4Q} \in \text{Sym}^{N'+1+4Q}(\mathcal{H} \otimes \mathcal{H}) \cap S_{(\bar{\mathcal{H}} \otimes \bar{\mathcal{H}})^{\otimes N'+1+4Q-2Q}}^n$ and let $\tilde{\rho}^{N'+1} = \text{Tr}_{4Q}[\tilde{\rho}^{N'+1+4Q}]$. Then, there exist a finite set \mathcal{V} of unit vectors $|v\rangle \in \bar{\mathcal{H}} \otimes \bar{\mathcal{H}}$, a probability distribution $\{p_v\}_{v \in \mathcal{V}}$ over \mathcal{V} , and almost-i.i.d. states $\tilde{\rho}_v^{N'+1} \in S_{v^{\otimes N'+1+4Q-8Q}}^{N'+1}$ such that

$$F\left(\tilde{\rho}^{N'+1}, \sum_{v \in \mathcal{V}} p_v \tilde{\rho}_v^{N'+1}\right) > 1 - Q^{(E+1)2t} \exp\left[-\frac{4Q(Q+1)}{N'+1+4Q}\right]. \quad (177)$$

Given a state $\rho^{N'+1+4Q} \in S_{\bar{\mathcal{H}}^{\otimes(N'+1+4Q-Q)}}^{N'+1+4Q}$, applying Theorem 7 to the purification $\tilde{\rho}^{N'+1+4Q}$ provided by Lemma 7 shows that the reduced state $\tilde{\rho}^{N'+1}$ is close in fidelity to a mixture of states that are i.i.d. on $N'+1-4Q$ subsystems. These results follow from the proof in the paper [61].

1.3 Hoeffding inequality for almost-i.i.d states

Given an almost i.i.d. state $|\Phi\rangle \in \mathcal{S}_{v^{\otimes t-r}}^t$, if we do heterodyne measurements over $t-m$ of the subsystems of $|\Phi\rangle$ and find the average over a function $f(\alpha)$, for our problem it is important to know how close will this statistical average be to the expectation value of this function over the Husimi Q function defined by $|v\rangle$. The following lemma gives this result [63]

Lemma 8. Let $M > 0 \in \mathbb{R}$ and let $f : \mathbb{C} \rightarrow \mathbb{R}$ be a function bounded as $|f(\alpha)| \leq M$ for all $\alpha \in \mathbb{C}^t$. Let $\mu > 0$ and $1 \leq m \leq r < t$ such that

$$(t-m)\mu > 2Mr. \quad (137)$$

Let also $|v\rangle \in \mathcal{H}$ and $|\Phi\rangle \in \mathcal{S}_{v^{\otimes t-r}}^t$. Let $\mathcal{M} = \{\mathcal{M}_\alpha\}_{\alpha \in \mathbb{C}^t}$ be a POVM on \mathcal{H} and let $D_{|v\rangle}$ be the probability density function of the outcomes of the measurement \mathcal{M} applied to $|v\rangle\langle v|$. Then

$$\Pr_\alpha \left[\left| \frac{1}{t-m} \sum_{i=1}^{t-m} f(\alpha_i) - \left(\mathbb{E}_{\beta \leftarrow D_{|v\rangle}} [f(\beta)] \right) \right| > \mu \right] \leq 2 \binom{t}{r} \exp \left[-\frac{t-r}{2} \left(\frac{\mu}{M} - \frac{2r}{t-m} \right)^2 \right], \quad (138)$$

where the probability is taken over the outcomes $\alpha = (\alpha_1, \dots, \alpha_{t-m})$ of the product measurement $\mathcal{M}^{\otimes t-m}$ applied to $|\Phi\rangle\langle\Phi|$.

Following the steps of Appendix 3.4 of [63], it is tedious but straightforward to prove Theorem 6 from here. □

J Efficiency of heterodyne verification: Proof of Theorem 4

The proof of Theorem 4 uses k -mode fidelity estimation as a subroutine with k -mode fidelity witness and statistical sampling inequality.

Let's first consider the case $\hat{S}(\xi)\hat{D}(\beta)\hat{U} = \mathbb{1}$, and therefore $\alpha = \gamma$, and our target state is $|\psi\rangle = \bigotimes_{i=1}^m |C_i\rangle$. For all $i \in \{1, \dots, m/k\}$, we write $|C_i\rangle = \sum_{\mathbf{n}=0}^{\mathbf{c}_i-1} \mathbf{c}_{i,\mathbf{n}} |\mathbf{n}\rangle$, where $\mathbf{c}_i \in (\mathbb{N}^*)^k$, and $\rho_i = \text{Tr}_{\{1, \dots, m\} \setminus \{ki-(k-1), \dots, ik\}}(\rho)$ the reduced state of ρ over the selected k modes. Then it is proven in Theorem 3 that

$$|F_{C_i}^{\text{real}}(\rho_i) - F_{C_i}^{\text{k-est}}(\tau_i)| \leq \lambda_i + \epsilon_{(\text{bias})}(\mathbf{C}_i, \mathbf{p}_i, \tau_i), \quad (178)$$

with probability $1 - \delta_i$, where $\delta_i = 2 \exp\left(-\frac{N\lambda_i^2}{2(R(\mathbf{C}_i, \mathbf{p}_i, \tau_i))^2}\right)$, and $\mathbf{p}_i = \{p_{ki-(k-1)}, \dots, p_{ki}\}$. Therefore, taking the union bound on probabilities

$$\left| 1 - \sum_{i=1}^{m/k} \left(1 - F(\rho_{ki-(k-1)\dots ik}, |\psi_{ki-(k-1)}\rangle \otimes \dots \otimes |\psi_{ki}\rangle) \right) - W_\psi^{(k)} \right|$$

$$\begin{aligned}
&= \left| \sum_{i=1}^{m/k} \left(F(\boldsymbol{\rho}_{ki-(k-1)\dots ki}, |\psi_{ki-(k-1)}\rangle \otimes \dots \otimes |\psi_{ki}\rangle) - F_{C_i}^{(k-est)}(\tau_i) \right) \right| \\
&\leq \sum_{i=1}^{m/k} \left| F(\boldsymbol{\rho}_{ki-(k-1)\dots ki}, |\psi_{ki-(k-1)}\rangle \otimes \dots \otimes |\psi_{ki}\rangle) - F_{C_i}^{(k-est)}(\tau_i) \right| \\
&\leq \sum_{i=1}^{m/k} (\lambda_i + \epsilon_{(\text{bias})}(\mathbf{C}_i, \mathbf{p}_i, \tau_i)). \tag{179}
\end{aligned}$$

with probability higher than $1 - P_W^{k-iid}$, where

$$P_W^{k-iid} := 2 \sum_{i=1}^{m/k} \exp\left(-\frac{N\lambda_i^2}{2(R(\mathbf{C}_i, \mathbf{p}_i, \tau_i))^2}\right). \tag{180}$$

Furthermore, using Eq. (14),

$$1 - \frac{m}{k}(1 - F(\boldsymbol{\rho}, |\psi\rangle)) \leq 1 - \sum_{i=1}^{m/k} \left(1 - F(\boldsymbol{\rho}_{ki-(k-1)\dots ki}, |\psi_{ki-(k-1)}\rangle \otimes \dots \otimes |\psi_{ki}\rangle)\right) \leq F(\boldsymbol{\rho}, |\psi\rangle). \tag{181}$$

Therefore,

$$1 - \frac{m}{k}(1 - F(\boldsymbol{\rho}, |\psi\rangle)) - \sum_{i=1}^{m/k} (\lambda_i + \epsilon_{(\text{bias})}(\mathbf{C}_i, \mathbf{p}_i, \tau_i)) \leq W_\psi^{(k)} \leq F(\boldsymbol{\rho}, |\psi\rangle) + \sum_{i=1}^{m/k} (\lambda_i + \epsilon_{(\text{bias})}(\mathbf{C}_i, \mathbf{p}_i, \tau_i)). \tag{182}$$

with probability higher than $1 - P_W^{k-iid}$, where P_W^{k-iid} is given by Eq. (180). Using the free parameters p_1, \dots, p_m and $\tau_1, \dots, \tau_{m/k}$, the errors and probabilities can be optimized.

We now generalize the previous proof to the case where the target state is of the form

$$|\psi\rangle = \hat{S}(\boldsymbol{\xi}) \hat{D}(\boldsymbol{\beta}) \hat{U} \bigotimes_{i=1}^m |C_i\rangle, \tag{183}$$

where for all $i \in \{1, \dots, m\}$ each of the states $|C_i\rangle = \sum_{n=0}^{c_i-1} c_{i,n} |n\rangle$ is a core state, where \hat{U} is an m -mode passive linear transformation with $m \times m$ unitary matrix U and where $\boldsymbol{\xi}, \boldsymbol{\beta} \in \mathbb{C}^m$. Using Lemma 5,

$$\text{Tr}(\hat{V}^\dagger \boldsymbol{\rho} \hat{V} \Pi_\alpha^0) = \text{Tr}(\boldsymbol{\rho} \hat{V} \Pi_\alpha^0 \hat{V}^\dagger) = \text{Tr}(\boldsymbol{\rho} \Pi_{U\alpha+\beta}^\xi). \tag{184}$$

Therefore, samples obtained from the unbalanced heterodyne sampling of $\boldsymbol{\rho}, \boldsymbol{\gamma}^{(1)}, \dots, \boldsymbol{\gamma}^{(N)}$ follow the same probability distribution as samples obtained from the balanced heterodyne sampling of $\hat{V}^\dagger \boldsymbol{\rho} \hat{V}, \boldsymbol{\alpha}^{(1)}, \dots, \boldsymbol{\alpha}^{(N)}$. Therefore, with classical post-processing $\boldsymbol{\alpha} = U^\dagger(\boldsymbol{\gamma} - \boldsymbol{\beta})$, we obtain a fidelity witness $W_\psi^{(k)}$, such that

$$\begin{aligned}
1 - \frac{m}{k}(1 - F(\hat{V}^\dagger \boldsymbol{\rho} \hat{V}, \bigotimes_{i=1}^m |C_i\rangle \langle C_i|)) - \sum_{i=1}^{m/k} (\lambda_i + \epsilon_{(\text{bias})}(\mathbf{C}_i, \mathbf{p}_i, \tau_i)) \\
\leq W_\psi^{(k)} \leq F(\hat{V}^\dagger \boldsymbol{\rho} \hat{V}, \bigotimes_{i=1}^m |C_i\rangle \langle C_i|) + \sum_{i=1}^{m/k} (\lambda_i + \epsilon_{(\text{bias})}(\mathbf{C}_i, \mathbf{p}_i, \tau_i)) \tag{185}
\end{aligned}$$

with probability higher than $1 - P_W^{k-iid}$, where P_W^{k-iid} is given by Eq. (180). Given that

$$F(\hat{V}^\dagger \boldsymbol{\rho} \hat{V}, \bigotimes_{i=1}^m |C_i\rangle \langle C_i|) = F(\boldsymbol{\rho}, |\psi\rangle \langle \psi|), \tag{186}$$

We have

$$1 - \frac{m}{k}(1 - F(\boldsymbol{\rho}, |\boldsymbol{\psi}\rangle \langle \boldsymbol{\psi}|)) - \sum_{i=1}^{m/k} (\lambda_i + \epsilon_{(\text{bias})}(\mathbf{C}_i, \mathbf{p}_i, \tau_i)) \leq W_{\boldsymbol{\psi}}^{(k)} \leq F(\boldsymbol{\rho}, |\boldsymbol{\psi}\rangle \langle \boldsymbol{\psi}|) + \sum_{i=1}^{m/k} (\lambda_i + \epsilon_{(\text{bias})}(\mathbf{C}_i, \mathbf{p}_i, \tau_i)). \quad (187)$$

K Verification of doped Gaussian states

To verify doped Gaussian states with the Gaussian unitaries restricted to passive linear transformations and displacement operators, we use a fidelity witness that is a combination of κt -mode fidelity witness and single mode witness $W_{\boldsymbol{\psi}}^{(\kappa t, 1)}$,

$$W^{(\kappa t, 1)} := 1 - (1 - F(\rho_{1, \dots, \kappa t}, \phi)) - \sum_{i=\kappa t+1}^m (1 - F(\rho_i, \psi_i)). \quad (188)$$

where $|\phi\rangle$ is a κt -mode quantum state.

Following the steps of the proof of Lemma 2, we can prove

$$\begin{aligned} & 1 - (m - \kappa t + 1)(1 - F(\rho, |\phi\rangle \otimes |\psi_{\kappa t+1}\rangle \otimes \dots \otimes |\psi_m\rangle)) \\ & \leq W^{(\kappa t, 1)} \leq F(\rho, |\phi\rangle \otimes |\psi_{\kappa t+1}\rangle \otimes \dots \otimes |\psi_m\rangle). \end{aligned} \quad (189)$$

Therefore, estimating $W^{(\kappa t, 1)}$ can give a lower bound on the fidelity between the output state $\boldsymbol{\rho}$ and the target state $|\boldsymbol{\psi}\rangle = S(\boldsymbol{\xi})D(\boldsymbol{\beta})\hat{U}|\phi\rangle \otimes |0\rangle^{\otimes m - \kappa t}$. Using this fidelity witness, a protocol to verify $|\boldsymbol{\psi}\rangle$ can be described as

Protocol 6. (*Fidelity witness estimation for t -doped Gaussian states*). We write $|\boldsymbol{\psi}\rangle = S(\boldsymbol{\xi})D(\boldsymbol{\beta})\hat{U}|\phi\rangle \otimes |0\rangle^{\otimes m - \kappa t}$ as the m -mode target pure state. Let $N \in \mathbb{N}^*$ and let $p_1, \dots, p_m \in \mathbb{N}^*$ and $0 < \tau_{\kappa t}, \tau_{\kappa t+1}, \dots, \tau_m < 1$ be free parameters. Let $\boldsymbol{\rho}^{\otimes N+1} = N+1$ copies of an unknown m -mode (mixed) quantum state $\boldsymbol{\rho}$.

1. Measure all m subsystems of N copies of $\boldsymbol{\rho}$ with unbalanced heterodyne detection with unbalancing parameters $\boldsymbol{\xi} = \{\xi_1, \dots, \xi_m\}$, obtaining the vectors of samples $\boldsymbol{\gamma}^{(1)}, \dots, \boldsymbol{\gamma}^{(N)} \in \mathbb{C}^m$.
2. For all $k \in \{1, \dots, N\}$, compute the vectors $\boldsymbol{\alpha}^{(k)} = U^\dagger(\boldsymbol{\gamma}^{(k)} - \boldsymbol{\beta})$. We write $\boldsymbol{\alpha}^{(k)} = (\alpha_1^{(k)}, \dots, \alpha_m^{(k)}) \in \mathbb{C}^m$.
3. Group the first κt -modes together and compute the mean $F_{\phi}^{(\kappa t - est)}$ of the function $z \mapsto g_{\phi}^{\kappa t - est}(z, \tau_{\kappa t})$ (defined in Eq. (41)) over the samples $\boldsymbol{\alpha}_{\kappa t}^{(1)}, \dots, \boldsymbol{\alpha}_{\kappa t}^{(N)} \in \mathbb{C}^{\kappa t}$, where $\boldsymbol{\alpha}_{\kappa t}^{(i)} = \{\alpha_1^{(i)}, \dots, \alpha_{\kappa t}^{(i)}\}$.
4. For all $i \in \{\kappa t + 1, \dots, m\}$, compute the mean F_{0_i} of the function $z \mapsto g_{0,0}^{(p_i)}(z, \tau_i)$ over the samples $\alpha_i^{(1)}, \dots, \alpha_i^{(N)} \in \mathbb{C}$.
5. Compute the fidelity witness estimate

$$W_{\boldsymbol{\psi}}^{(\kappa t, 1)} = 1 - (1 - F_{\phi}^{(t - est)}) - \sum_{i=\kappa t+1}^m (1 - F_{0_i}). \quad (190)$$

Theorem 8. Let $\epsilon, \delta > 0$. With the notations of Protocol 6, it is always possible to find N such that for $N \geq N_{\text{threshold}}$

$$1 - (m - \kappa t + 1)(1 - F(\rho, |\phi\rangle \otimes |\psi_{\kappa t+1}\rangle \otimes \cdots \otimes |\psi_m\rangle)) - \epsilon \leq W_{\psi}^{(\kappa t, 1)} \leq F(\rho, |\phi\rangle \otimes |\psi_{\kappa t+1}\rangle \otimes \cdots \otimes |\psi_m\rangle) + \epsilon, \quad (191)$$

with probability $1 - \delta$, ϵ and δ are given by

$$\epsilon = \lambda_{\kappa t} + \epsilon_{\text{bias}}(\phi, \mathbf{p}_{\kappa t}, \tau_{\kappa t}) + \sum_{i=\kappa t+1}^m (\lambda_i + \tau_i^{p_i} A_{0_i}^{(p_i)}), \quad (192)$$

$$\delta = 2 \exp \left[-\frac{N \lambda_{\kappa t}}{2(R(\phi, \mathbf{p}_{\kappa t}, \tau_{\kappa t}))^2} \right] + 2 \sum_{i=\kappa t+1}^m \exp \left[-\frac{N \tau_i^2 \lambda_i^2}{2(B_C^{p_i}(\tau_i))^2} \right]. \quad (193)$$

Proof. The proof of Theorem 8 combines Theorem 3 with Eq. (189) and Hoeffding inequality (Lemma 1).

We will prove the Theorem for $\hat{S}(\boldsymbol{\xi})\hat{D}(\boldsymbol{\beta})\hat{U} = \mathbb{1}$, the extension to any arbitrary $\hat{S}(\boldsymbol{\xi})\hat{D}(\boldsymbol{\beta})\hat{U}(|\phi\rangle \otimes |0\rangle^{\otimes(m-\kappa t)})$ can be done following the same steps as in the proof of Theorem 4.

Our target state is $|\boldsymbol{\psi}\rangle = |\phi\rangle \otimes |0\rangle^{\otimes(m-\kappa t)}$. For the first κt modes, if $\boldsymbol{\rho}_{\kappa t}$ denotes the reduced state over the first κt modes, then from theorem 3,

$$|F_{\phi}(\boldsymbol{\rho}_{\kappa t}) - F_{\phi}^{k\text{-est}}(\tau_{\kappa t})| \leq \lambda_{\kappa t} + \epsilon_{\text{bias}}(\phi, \mathbf{p}_{\kappa t}, \tau_{\kappa t}), \quad (194)$$

with probability $1 - \delta_{\kappa t}$, where $\delta_{\kappa t} = 2 \exp \left(-\frac{N \lambda_{\kappa t}}{2(R(\phi, \mathbf{p}_{\kappa t}, \tau_{\kappa t}))^2} \right)$, and $\mathbf{p}_{\kappa t} = \{p_1, \dots, p_{\kappa t}\}$. Furthermore, for $i = \{\kappa t + 1, \dots, m\}$, if $\boldsymbol{\rho}_i$ denotes the reduced state over the i^{th} mode, then from appendix C of [51],

$$|F(|0\rangle_i, \boldsymbol{\rho}_i) - F_{0_i}(\tau_i)| \leq \lambda_i + \tau_i^{p_i} A_{0_i}^{(p_i)}, \quad (195)$$

with probability $1 - \delta_i$, where $\delta_i = 2 \exp \left(-\frac{N \lambda_i^2 \tau_i^2}{2(B_{0_i}^{(p_i)}(\tau_i))^2} \right)$. $A_{0_i}^{(p_i)}$ and $B_{0_i}^{(p_i)}(\tau_i)$ is given by

$$A_{0_i}^{(p_i)} = 1, \quad (196)$$

$$B_{0_i}^{(p_i)}(\tau_i) = \tau_i^{-1} \binom{p_i + 1}{p_i - 1}. \quad (197)$$

Therefore, taking the union bound on probabilities,

$$\begin{aligned} & \left| 1 - (1 - F(|\phi\rangle, \boldsymbol{\rho}_{1, \dots, \kappa t})) - \sum_{i=\kappa t+1}^m 1 - F(|0\rangle_i, \boldsymbol{\rho}_i) - W_{\psi}^{\kappa t, 1} \right| \\ &= \left| (F(|\phi\rangle, \boldsymbol{\rho}_{1, \dots, \kappa t}) - F_{\phi}^{(t\text{-est})}(\tau_{\kappa t})) + \sum_{i=\kappa t+1}^m (F(|0\rangle_i, \boldsymbol{\rho}_i) - F_{0_i}(\tau_i)) \right| \\ &\leq |F(|\phi\rangle, \boldsymbol{\rho}_{1, \dots, \kappa t}) - F_{\phi}^{(t\text{-est})}(\tau_{\kappa t})| + \sum_{i=\kappa t+1}^m |F(|0\rangle_i, \boldsymbol{\rho}_i) - F_{0_i}(\tau_i)| \\ &\leq \lambda_{\kappa t} + \epsilon_{\text{bias}}(\phi, \mathbf{p}_{\kappa t}, \tau_{\kappa t}) + \sum_{i=\kappa t+1}^m (\lambda_i + \tau_i^{p_i} A_{0_i}^{(p_i)}). \end{aligned} \quad (198)$$

with probability higher than $1 - P_W^{k\text{-i.i.d.}}$, where

$$P_W^{k\text{-i.i.d.}} = 2 \exp \left(-\frac{N \lambda_{\kappa t}^2}{2(R(\phi, \mathbf{p}_{\kappa t}, \tau_{\kappa t}))^2} \right) + 2 \sum_{i=\kappa t+1}^m \exp \left(-\frac{N \tau_i^2 \lambda_i^2}{2(B_{0_i}^{(p_i)}(\tau_i))^2} \right). \quad (199)$$

Furthermore, using Eq. (189),

$$1 - (m - \kappa t + 1)F(|\phi\rangle \otimes |\psi_{\kappa t+1}\rangle \otimes \cdots \otimes |\psi_m\rangle, \boldsymbol{\rho}) \leq W^{(\kappa t, 1)} \leq F(|\phi\rangle \otimes |\psi_{\kappa t+1}\rangle \otimes \cdots \otimes |\psi_m\rangle, \boldsymbol{\rho}). \quad (200)$$

Therefore,

$$\begin{aligned} 1 - (m - \kappa t + 1)F(|\phi\rangle \otimes |\psi_{\kappa t+1}\rangle \otimes \cdots \otimes |\psi_m\rangle, \boldsymbol{\rho}) - (\lambda_{\kappa t} + \epsilon_{\text{bias}}(\phi, \mathbf{p}_{\kappa t}, \tau_{\kappa t}) + \sum_{i=\kappa t+1}^m (\tau^{p_i} + A_{0_i}^{(p_i)})) \\ \leq W_{\psi}^{(\kappa t, 1)} \leq F(|\phi\rangle \otimes |\psi_{\kappa t+1}\rangle \otimes \cdots \otimes |\psi_m\rangle, \boldsymbol{\rho}) + \lambda_{\kappa t} + \epsilon_{\text{bias}}(\phi, \mathbf{p}_{\kappa t}, \tau_{\kappa t}) + \sum_{i=\kappa t+1}^m (\tau^{p_i} + A_{0_i}^{(p_i)}), \end{aligned} \quad (201)$$

with probability higher than $1 - P_W^{k-i.i.d.}$, where $P_W^{k-i.i.d.}$ is given by Eq. (199). \square

Using the free parameters p_1, \dots, p_m and $\tau_{\kappa t}, \tau_{\kappa t+1}, \dots, \tau_m$, the number of samples required to obtain the desired precision with the desired probability can be optimized. Asymptotically, $N_{\text{threshold}}$ scales as

$$N_{\text{threshold}} = \tilde{\mathcal{O}} \left(\frac{(\text{constant})^{\kappa t}}{\epsilon^2} \log \left(\frac{1}{\delta} \right) \right) \quad (202)$$

where $\tilde{\mathcal{O}}$ represents ordering upto terms polynomial in $m, \kappa t$ and ϵ .

Therefore, Protocol 6 allows us to verify a doped Gaussian state with heterodyne sampling using multimode fidelity witness. This certification is not possible using the witness based on single-mode fidelities ($k = 1$), since the state $|\phi\rangle$ maybe possibly be entangled.

L Noisy heterodyne estimator

We denote by $\mathbb{E}_{\alpha \leftarrow D}[f(\alpha)]$ the expected value of a function f for samples drawn from a distribution D . We write $\eta \in (0, 1]$ the quantum efficiency of the heterodyne detection. The corresponding probability distribution is related to the smoothed Husimi Q function:

$$W(\alpha, s) = -\frac{2}{1+s} \int_{\beta \in \mathbb{C}} Q(\beta) e^{\frac{2}{1+s}|\alpha-\beta|^2} \frac{d^2\beta}{\pi}, \quad (203)$$

for all $\alpha \in \mathbb{C}$, where $s = 1 - 2\eta^{-1} \leq -1$ [70]. The noisy heterodyne probability distribution is then given by $\frac{1}{\eta} W(\frac{\alpha}{\sqrt{\eta}}, s)$. In particular, dividing a sample of lossy heterodyne detection by $\sqrt{\eta}$ gives a complex number sampled from $W(\alpha, s)$. Let us introduce for $k, l \geq 0$ the polynomials

$$\begin{aligned} \mathcal{L}_{k,l}(z) &:= e^{zz^*} \frac{(-1)^{k+l}}{\sqrt{k!}\sqrt{l!}} \frac{\partial^{k+l}}{\partial z^k \partial z^{*l}} e^{-zz^*} \\ &= \sum_{p=0}^{\min(k,l)} \frac{\sqrt{k!}\sqrt{l!}(-1)^p}{p!(k-p)!(l-p)!} z^{l-p} z^{*k-p}, \end{aligned} \quad (204)$$

for $z \in \mathbb{C}$, which are, up to a normalisation, the Laguerre 2D polynomials. These polynomials allow us to write a developed expression for the generalised quasiprobability distribution of a state $\rho = \sum_{m,n \geq 0} \rho_{mn} |m\rangle\langle n|$ [71] (note that the generalised quasiprobability distributions in this reference are parametrized by a parameter r which is related to our parametrization by $r = -s$): for all $s < 1$ and all $\alpha \in \mathbb{C}$,

$$W_{\rho}(\alpha, s) = \sum_{m,n \geq 0} \rho_{mn} W_{|m\rangle\langle n|}(\alpha, s), \quad (205)$$

where for all $m, n \in \mathbb{N}$,

$$\begin{aligned} W_{|m\rangle\langle n|}(\alpha, s) &= \frac{2}{\pi} \left(\frac{1+s}{1-s} \right)^{\frac{m+n}{2}} e^{-\frac{2}{1-s}|\alpha|^2} \mathcal{L}_{m,n} \left(\frac{2\alpha}{\sqrt{1-s^2}} \right) \\ &= \frac{1}{\pi} \left(\frac{2}{1-s} \right)^{m+n+1} e^{-\frac{2}{1-s}|\alpha|^2} \sum_{q=0}^{\min(m,n)} \frac{\sqrt{m!}\sqrt{n!}(-1)^q}{q!(m-q)!(n-q)!} \left(\frac{1-s^2}{4} \right)^q \alpha^{n-q} \alpha^{*m-q}. \end{aligned} \quad (206)$$

Additionally, for all $k, l \in \mathbb{N}$, we define with these polynomials the functions

$$\begin{aligned} f_{k,l}(z) &:= \frac{1}{\eta^{k+l+1} \tau^{\frac{k+l}{2}+1}} e^{(\eta-\frac{1}{\tau})zz^*} \mathcal{L}_{l,k} \left(\frac{z}{\sqrt{\tau}} \right) \\ &= \frac{1}{(\tau\eta)^{k+l+1}} e^{(\eta-\frac{1}{\tau})zz^*} \sum_{p=0}^{\min(k,l)} \frac{\sqrt{k!}\sqrt{l!}(-1)^p \tau^p}{p!(k-p)!(l-p)!} z^{k-p} z^{*l-p}, \end{aligned} \quad (207)$$

for all $z \in \mathbb{C}$ and all $0 < \tau < \frac{1}{\eta}$, which may be thought of as regularized Glauber–Sudarshan P functions of Fock basis operators [63, 72]. The function $f_{k,l}$, being a polynomial multiplied by a converging Gaussian function, is bounded over \mathbb{C} .

We obtain the following result:

Lemma 9. *Let $s = 1 - 2\eta^{-1} \leq -1$, let $k, l \in \mathbb{N}$ and let $0 < \tau < \frac{1}{\eta}$. Let $\rho = \sum_{m,n \geq 0} \rho_{mn} |m\rangle\langle n|$ be a density operator. Then,*

$$\mathbb{E}_{\alpha \leftarrow W_\rho(\alpha, s)} [f_{k,l}] = \rho_{kl} + \sum_{j=1}^{+\infty} \rho_{k+j, l+j} (1 - \eta + \tau\eta^2)^j \sqrt{\binom{j+k}{k} \binom{j+l}{l}}. \quad (208)$$

where the function $f_{k,l}$ is defined in Eq. (207).

Proof. We first prove the Lemma without caring about convergence of the sums, and justify these afterwards. We have

$$\begin{aligned} \mathbb{E}_{\alpha \leftarrow W_\rho(\alpha, s)} [f_{k,l}] &= \int f_{k,l}(\alpha) W_\rho(\alpha, s) d^2\alpha \\ &= \sum_{m,n \geq 0} \rho_{mn} \int f_{k,l}(\alpha) W_{|m\rangle\langle n|}(\alpha, s) d^2\alpha \\ &= \sum_{m,n \geq 0} \rho_{mn} \sum_{q=0}^{\min(m,n)} \left(\frac{2}{1-s} \right)^{m+n+1} \frac{\sqrt{m!}\sqrt{n!}(-1)^q}{q!(m-q)!(n-q)!} \left(\frac{1-s^2}{4} \right)^q \frac{1}{(\tau\eta)^{k+l+1}} \sum_{p=0}^{\min(k,l)} \frac{\sqrt{k!}\sqrt{l!}(-1)^p \tau^p}{p!(k-p)!(l-p)!} \\ &\quad \times \int \alpha^{n-q} \alpha^{*m-q} \alpha^{k-p} \alpha^{*l-p} e^{-\frac{2}{1-s}|\alpha|^2} e^{(\eta-\frac{1}{\tau})|\alpha|^2} \frac{d^2\alpha}{\pi}. \end{aligned} \quad (209)$$

With $s = 1 - 2\eta^{-1}$, the integral in the last line can be computed as

$$\int \alpha^{n-q+k-p} \alpha^{*m-q+l-p} e^{-\frac{|\alpha|^2}{\tau}} \frac{d^2\alpha}{\pi} = \left(\frac{m+n+k+l}{2} - p - q \right)! \tau^{\frac{m+n+k+l}{2} - p - q + 1} \delta_{m-k, n-l}. \quad (210)$$

where δ is the Kronecker symbol, and where we used polar coordinates $d^2\alpha = r dr d\theta$ with $\int_0^{2\pi} e^{ia\theta} d\theta = 2\pi\delta_{a,0}$ and $\int_{\mathbb{R}} r^{2N+1} e^{-\frac{r^2}{\tau}} dr = \frac{1}{2} N! \tau^{N+1}$ for $N = \frac{m+n+k+l}{2} - p - q$. The expression in Eq. (209) thus

reduces to:

$$\begin{aligned}
\mathbb{E}_{\alpha \leftarrow W_\rho(\alpha, s)}[f_{k,l}] &= \sum_{\substack{m, n \geq 0 \\ m-k=n-l}} \rho_{mn} \sum_{q=0}^{\min(m,n)} \left(\frac{2}{1-s}\right)^{m+n+1} \frac{\sqrt{m!}\sqrt{n!}(-1)^q}{q!(m-q)!(n-q)!} \left(\frac{1-s^2}{4}\right)^q \frac{1}{(\tau\eta)^{k+l+1}} \\
&\quad \times \sum_{p=0}^{\min(k,l)} \frac{\sqrt{k!}\sqrt{l!}(-1)^p \tau^p}{p!(k-p)!(l-p)!} \left(\frac{m+n+k+l}{2} - p - q\right)! \tau^{\frac{m+n+k+l}{2} - p - q + 1} \\
&= \sum_{\substack{m, n \geq 0 \\ m-k=n-l}} \rho_{mn} \sum_{q=0}^{\min(m,n)} \left(\frac{2}{1-s}\right)^{m+n+1} \frac{\sqrt{m!}\sqrt{n!}(-1)^q}{q!(m-q)!(n-q)!} \left(\frac{1-s^2}{4}\right)^q \frac{\tau^{\frac{m+n-k-l}{2} - q}}{\eta^{k+l+1}} \\
&\quad \times \frac{\left(\frac{m+n+k+l}{2} - q\right)!}{\sqrt{k!}\sqrt{l!}} \sum_{p=0}^{\min(k,l)} (-1)^p \frac{\binom{k}{p}\binom{l}{p}}{\binom{\frac{m+n+k+l}{2} - q}{p}} \\
&= \sum_{\substack{m, n \geq 0 \\ m-k=n-l}} \rho_{mn} \sum_{q=0}^{\min(m,n)} (\tau\eta^2)^{\frac{m+n-k-l}{2} - q} \frac{\sqrt{m!}\sqrt{n!}}{q!(m-q)!(n-q)!} (1-\eta)^q \\
&\quad \times \frac{\left(\frac{m+n+k+l}{2} - q\right)!}{\sqrt{k!}\sqrt{l!}} \sum_{p=0}^{\min(k,l)} (-1)^p \frac{\binom{k}{p}\binom{l}{p}}{\binom{\frac{m+n+k+l}{2} - q}{p}},
\end{aligned} \tag{211}$$

where we used $\frac{2}{1-s} = \eta$ and $\frac{1-s^2}{4} = -\frac{1-\eta}{\eta^2}$ in the fifth line. Now the last sum is given by (see result 7.1 of [73]):

$$\sum_{p=0}^{\min(k,l)} (-1)^p \frac{\binom{k}{p}\binom{l}{p}}{\binom{\frac{m+n+k+l}{2} - q}{p}} = \begin{cases} \frac{\left(\frac{m+n+k-l}{2} - q\right)! \left(\frac{m+n-k+l}{2} - q\right)!}{\left(\frac{m+n+k+l}{2} - q\right)! \left(\frac{m+n-k-l}{2} - q\right)!} & \text{for } \frac{m+n+k+l}{2} - q \geq k+l, \\ 0 & \text{for } \frac{m+n+k+l}{2} - q < k+l. \end{cases} \tag{212}$$

In particular, with the condition $m - k = n - l$, having $q \geq 0$ implies $m \geq k$ and $n \geq l$. We thus obtain

$$\begin{aligned}
\mathbb{E}_{\alpha \leftarrow W_\rho(\alpha, s)}[f_{k,l}] &= \sum_{\substack{m \geq k, n \geq l \\ m-k=n-l}} \rho_{mn} \sum_{q=0}^{\min(m,n)} (\tau\eta^2)^{\frac{m+n-k-l}{2} - q} \frac{\sqrt{m!}\sqrt{n!}}{q!(m-q)!(n-q)!} (1-\eta)^q \frac{\left(\frac{m+n+k-l}{2} - q\right)! \left(\frac{m+n-k+l}{2} - q\right)!}{\sqrt{k!}\sqrt{l!} \left(\frac{m+n-k-l}{2} - q\right)!} \\
&= \sum_{j \geq 0} \rho_{j+k, j+l} \sum_{q=0}^j (\tau\eta^2)^{j-q} \frac{\sqrt{(j+k)!}\sqrt{(j+l)!}}{q!(j+k-q)!(j+l-q)!} (1-\eta)^q \frac{(j+k-q)!(j+l-q)!}{\sqrt{k!}\sqrt{l!} (j-q)!} \\
&= \sum_{j \geq 0} \rho_{j+k, j+l} (\tau\eta^2)^j \sqrt{\binom{j+k}{k} \binom{j+l}{l}} \sum_{q=0}^j \binom{j}{q} \left(\frac{1-\eta}{\tau\eta^2}\right)^q \\
&= \sum_{j \geq 0} \rho_{j+k, j+l} (1-\eta + \tau\eta^2)^j \sqrt{\binom{j+k}{k} \binom{j+l}{l}} \\
&= \rho_{k,l} + \sum_{j \geq 1} \rho_{j+k, j+l} (1-\eta + \tau\eta^2)^j \sqrt{\binom{j+k}{k} \binom{j+l}{l}},
\end{aligned} \tag{213}$$

where we have set $j = m - k = n - l$ in the second line.

We now consider the convergence of the above expressions. The interversion of sums and integral in Eq. (209) is valid if the series in Eq. (213) converges. Let $t := 1 - \eta + \tau\eta^2$. Since $0 < \eta \leq 1$ and

$0 < \tau < \frac{1}{\eta}$, we have $0 < t < 1$. The term $\sqrt{\binom{j+k}{k}\binom{j+l}{l}}$ is bounded by a polynomial in j , so the function $j \mapsto t^j \sqrt{\binom{j+k}{k}\binom{j+l}{l}}$ is bounded over \mathbb{N} . Writing M its maximum, we obtain for all $N \in \mathbb{N}$:

$$\begin{aligned}
\left| \sum_{j=0}^N \rho_{j+k,j+l} (1 - \eta + \tau\eta^2)^j \sqrt{\binom{j+k}{k}\binom{j+l}{l}} \right| &\leq M \sum_{j=0}^N |\rho_{j+k,j+l}| \\
&\leq M \sum_{j=0}^N \sqrt{\rho_{j+k,j+k}} \sqrt{\rho_{j+l,j+l}} \\
&\leq M \sqrt{\sum_{j=0}^N \rho_{j+k,j+k} \sum_{j=0}^N \rho_{j+l,j+l}} \\
&\leq M,
\end{aligned} \tag{214}$$

where we used the fact that ρ is positive semidefinite in the second line, Cauchy-Schwartz inequality in the third line and $\text{Tr}(\rho) = 1$ in the last line. Taking $N \rightarrow +\infty$ completes the proof. \square

We may thus use the bounded functions $f_{k,l}$ to estimate density matrix elements using noisy heterodyne detection, with an error quantified by Lemma 9. Noticing that the error term for the coefficient (k,l) only depends on higher coefficients, we take linear combinations of these estimators in order to “push” the error to higher coefficients. Namely, for $0 < \tau < \frac{1}{\eta}$, writing $t = 1 - \eta + \tau\eta^2$, we define for all $p \in \mathbb{N}^*$ and all $z \in \mathbb{C}$:

$$g_{k,l}^{p(\text{het})}(z, \eta, \tau) := \sum_{j=0}^{p-1} (-1)^j f_{k+j,l+j}(z) t^j \sqrt{\binom{j+k}{k}\binom{j+l}{l}}. \tag{215}$$

We obtain the following result:

Lemma 10. *Let $s = 1 - 2\eta^{-1} \leq -1$, let $k, l \in \mathbb{N}$, let $p \in \mathbb{N}^*$, let $0 < \tau < \frac{1}{\eta}$ and let $t = 1 - \eta + \tau\eta^2$. Let $\rho = \sum_{m,n \geq 0} \rho_{mn} |m\rangle\langle n|$ be a density operator. Then,*

$$\mathbb{E}_{\alpha \leftarrow W_\rho(\alpha, s)} [g_{k,l}^{(p)}] = \rho_{kl} + (-1)^{p+1} \sum_{q=p}^{+\infty} \rho_{k+q,l+q} t^q \binom{q-1}{p-1} \sqrt{\binom{k+q}{k}\binom{l+q}{l}}. \tag{216}$$

where the function $g_{k,l}$ is defined in Eq. (215).

The proof is identical to the case $\eta = 1$, by replacing τ with $t = 1 - \eta + \tau\eta^2$ and $Q_\rho(\alpha)$ by $W_\rho(\alpha, s)$, with $s = 1 - 2\eta^{-1}$. We reproduce it below for completeness:

Proof. We prove the lemma by induction on $p \in \mathbb{N}^*$. By Lemma 9 we have, for all single-mode (mixed) state $\rho = \sum_{i,j \geq 0} \rho_{ij} |i\rangle\langle j|$, for all $k, l \in \mathbb{N}$

$$\mathbb{E}_{\alpha \leftarrow W_\rho(\alpha, s)} [f_{k,l}] = \rho_{kl} + \sum_{q=1}^{+\infty} \rho_{k+q,l+q} t^q \sqrt{\binom{k+q}{k}\binom{l+q}{l}}. \tag{217}$$

With Eq. (215), this gives

$$\mathbb{E}_{\alpha \leftarrow W_\rho(\alpha, s)} [g_{k,l}^{(1)}] = \rho_{kl} + \sum_{q=1}^{+\infty} \rho_{k+q,l+q} t^q \sqrt{\binom{k+q}{k}\binom{l+q}{l}}, \tag{218}$$

hence the lemma is proven for $p = 1$ since $\binom{q-1}{0} = 1$.

Assuming the lemma holds for some $p \in \mathbb{N}^*$,

$$\begin{aligned}
\mathbb{E}_{\alpha \leftarrow W_\rho(\alpha, s)} [g_{k, l}^{(p)}] &= \rho_{kl} + (-1)^{p+1} \sum_{q=p}^{+\infty} \rho_{k+q, l+q} t^q \binom{q-1}{p-1} \sqrt{\binom{k+q}{k} \binom{l+q}{l}} \\
&= \rho_{kl} + (-1)^{p+1} \rho_{k+p, l+p} t^p \sqrt{\binom{k+p}{k} \binom{l+p}{l}} \\
&\quad + (-1)^{p+1} \sum_{q=p+1}^{+\infty} \rho_{k+q, l+q} t^q \binom{q-1}{p-1} \sqrt{\binom{k+q}{k} \binom{l+q}{l}}.
\end{aligned} \tag{219}$$

Now by Eq. (217), with $k = k + p$ and $l = l + p$, we have

$$\mathbb{E}_{\alpha \leftarrow W_\rho(\alpha, s)} [f_{k+p, l+p}] = \rho_{k+p, l+p} + \sum_{q=1}^{+\infty} \rho_{k+q+p, l+q+p} t^q \sqrt{\binom{k+q+p}{k+p} \binom{l+q+p}{l+p}}, \tag{220}$$

so that

$$\begin{aligned}
\mathbb{E}_{\alpha \leftarrow W_\rho(\alpha, s)} [g_{k, l}^{(p+1)}] &= \mathbb{E}_{\alpha \leftarrow W_\rho(\alpha, s)} \left[g_{k, l}^{(p)} + (-1)^p t^p \sqrt{\binom{k+p}{k} \binom{l+p}{l}} f_{k+p, l+p} \right] \\
&= \rho_{kl} + (-1)^{p+1} \rho_{k+p, l+p} t^p \sqrt{\binom{k+p}{k} \binom{l+p}{l}} \\
&\quad + (-1)^{p+1} \sum_{q=p+1}^{+\infty} \rho_{k+q, l+q} t^q \binom{q-1}{p-1} \sqrt{\binom{k+q}{k} \binom{l+q}{l}} \\
&\quad + (-1)^p t^p \sqrt{\binom{k+p}{k} \binom{l+p}{l}} \rho_{k+p, l+p} \\
&\quad + (-1)^p t^p \sqrt{\binom{k+p}{k} \binom{l+p}{l}} \sum_{q=1}^{+\infty} \rho_{k+q+p, l+q+p} t^q \sqrt{\binom{k+q+p}{k+p} \binom{l+q+p}{l+p}} \\
&= \rho_{kl} + (-1)^{p+1} \sum_{q=p+1}^{+\infty} \rho_{k+q, l+q} t^q \binom{q-1}{p-1} \sqrt{\binom{k+q}{k} \binom{l+q}{l}} \\
&\quad + (-1)^p t^p \sqrt{\binom{k+p}{k} \binom{l+p}{l}} \sum_{q=1}^{+\infty} \rho_{k+q+p, l+q+p} t^q \sqrt{\binom{k+q+p}{k+p} \binom{l+q+p}{l+p}} \\
&= \rho_{kl} + (-1)^{p+1} \sum_{q=p+1}^{+\infty} \rho_{k+q, l+q} t^q \binom{q-1}{p-1} \sqrt{\binom{k+q}{k} \binom{l+q}{l}} \\
&\quad + (-1)^p \sqrt{\binom{k+p}{k} \binom{l+p}{l}} \sum_{q=p+1}^{+\infty} \rho_{k+q, l+q} t^q \sqrt{\binom{k+q}{k+p} \binom{l+q}{l+p}} \\
&= \rho_{kl} + (-1)^{p+2} \sum_{q=p+1}^{+\infty} \rho_{k+q, l+q} t^q \\
&\quad \times \left[\sqrt{\binom{k+p}{k} \binom{l+p}{l} \binom{k+q}{k+p} \binom{l+q}{l+p}} - \binom{q-1}{p-1} \sqrt{\binom{k+q}{k} \binom{l+q}{l}} \right].
\end{aligned} \tag{221}$$

We have

$$\begin{aligned}
\binom{k+p}{k} \binom{l+p}{l} \binom{k+q}{k+p} \binom{l+q}{l+p} &= \frac{(k+p)!(l+p)!(k+q)!(l+q)!}{k!p!l!p!(k+p)!(q-p)!(l+p)!(q-p)!} \\
&= \frac{(k+q)!(l+q)!}{k!(k+p)!p!^2(q-p)!^2} \\
&= \binom{q}{p}^2 \binom{k+q}{k} \binom{l+q}{l},
\end{aligned} \tag{222}$$

so the last expression in Eq. (221) simplifies as

$$\begin{aligned}
\mathbb{E}_{\alpha \leftarrow W_\rho(\alpha, s)} [g_{k,l}^{(p+1)}] &= \rho_{kl} + (-1)^{p+2} \sum_{q=p+1}^{+\infty} \rho_{k+q, l+q} t^q \sqrt{\binom{k+q}{k} \binom{l+q}{l}} \left[\binom{q}{p} - \binom{q-1}{p-1} \right] \\
&= \rho_{kl} + (-1)^{p+2} \sum_{q=p+1}^{+\infty} \rho_{k+q, l+q} t^q \binom{q-1}{p} \sqrt{\binom{k+q}{k} \binom{l+q}{l}},
\end{aligned} \tag{223}$$

which completes the proof. Note that the convergence of the series in the right hand side directly follows from the convergence of the series in the error term of Lemma 9, since it is obtained as the sum of p such series. □

The practical differences between the cases $\eta = 1$ and $\eta < 1$ stem from two points:

- the parameter $0 < \tau < 1$ is replaced by $t = 1 - \eta + \tau\eta^2$, with $1 - \eta < t < 1$, so the optimisation region for this parameter is smaller;
- the definition of the functions f and g are modified, which affects their range.

For the functions f , this last point can be made more precise: writing explicitly the dependence in τ , we obtain with Eq. (207):

$$f_{k,l}^{\text{noisy}} \left(\frac{z}{\sqrt{\eta}}, \frac{\tau}{\eta} \right) = \frac{1}{\eta^{\frac{k+l}{2}}} f_{k,l}^{\text{ideal}}(z, \tau), \tag{224}$$

which shows that the overhead due to the imperfect detection is given by a factor $\frac{1}{\eta^{\frac{k+l}{2}}}$ in the range of the estimator, and thus with Hoeffding inequality by a factor $\frac{1}{\eta^{k+l}}$ in the number of samples needed for the same confidence interval. In practice this only gives a rough estimate since the optimised parameter is t and not τ , and since the functions used are the g functions and not the f functions. In any case, we expect the number of samples needed to increase as the quantum efficiency decreases, since we are seeking the same information from a more noisy distribution.

An immediate application of Lemma 10 gives

$$\begin{aligned}
\left| \mathbb{E}_{\alpha \leftarrow W_\rho(\alpha, s)}[g_{k,l}^{(p)}] - \rho_{kl} \right| &\leq \sum_{q=p}^{+\infty} |\rho_{k+q, l+q}| t^q \binom{q-1}{p-1} \sqrt{\binom{k+q}{k} \binom{l+q}{l}} \\
&\leq \max_{q \geq p} \left(t^q \binom{q-1}{p-1} \sqrt{\binom{k+q}{k} \binom{l+q}{l}} \right) \sum_{q=p}^{+\infty} |\rho_{k+q, l+q}| \\
&\leq \max_{q \geq p} \left(t^q \binom{q-1}{p-1} \sqrt{\binom{k+q}{k} \binom{l+q}{l}} \right) \sum_{q=p}^{+\infty} \sqrt{\rho_{k+q, k+q}} \sqrt{\rho_{l+q, l+q}} \\
&\leq \max_{q \geq p} \left(t^q \binom{q-1}{p-1} \sqrt{\binom{k+q}{k} \binom{l+q}{l}} \right) \sqrt{\sum_{q=p}^{+\infty} \rho_{k+q, k+q} \sum_{q=p}^{+\infty} \rho_{l+q, l+q}} \\
&\leq \max_{q \geq p} \left(t^q \binom{q-1}{p-1} \sqrt{\binom{k+q}{k} \binom{l+q}{l}} \right),
\end{aligned} \tag{225}$$

where we used the fact that ρ is positive semidefinite in the third line, Cauchy–Schwarz inequality in the fourth line, and $\text{Tr}(\rho) = 1$ in the last line. This last bound is tight: if $p_{k,l} \geq p$ is the integer achieving the maximum in the last equation, then the inequality is an equality for $\rho = |p_{k,l}\rangle\langle p_{k,l}|$. We have

$$\begin{aligned}
t^{q+1} \binom{q}{p-1} \sqrt{\binom{k+q+1}{k} \binom{l+q+1}{l}} &\stackrel{\leq}{\geq} t^q \binom{q-1}{p-1} \sqrt{\binom{k+q}{k} \binom{l+q}{l}} \\
&\Leftrightarrow t \stackrel{\leq}{\geq} \frac{q-p+1}{q} \sqrt{\binom{q+1}{k+q+1} \binom{q+1}{l+q+1}} \\
&\Leftrightarrow t \stackrel{\leq}{\geq} \left(1 - \frac{p-1}{q}\right) \sqrt{1 - \frac{k}{k+q+1}} \sqrt{1 - \frac{l}{l+q+1}},
\end{aligned} \tag{226}$$

where the right hand side in the last line is an increasing function of q . Hence, the function $q \mapsto t^q \binom{q-1}{p-1} \sqrt{\binom{k+q}{k} \binom{l+q}{l}}$ is monotonically increasing to its maximum and then monotonically decreasing, and its maximum is attained for the first integer $p_{k,l}$ greater or equal to p such that $t \leq \left(1 - \frac{p-1}{p_{k,l}}\right) \sqrt{1 - \frac{k}{k+p_{k,l}+1}} \sqrt{1 - \frac{l}{l+p_{k,l}+1}}$. The bound above then gives

$$\left| \mathbb{E}_{\alpha \leftarrow W_\rho(\alpha, s)}[g_{k,l}^{(p)}] - \rho_{kl} \right| \leq t^{p_{k,l}} \binom{p_{k,l}-1}{p-1} \sqrt{\binom{k+p_{k,l}}{k} \binom{l+p_{k,l}}{l}}. \tag{227}$$